GeoHazards

MDPI

Article

Towards a Modern and Sustainable Sediment Management Plan in Mountain Catchment

Alessio Cislaghi [1,2,*], Emanuele Morlotti [1], Vito Giuseppe Sacchetti [3], Dario Bellingeri [3] and Gian Battista Bischetti [1,2]

[1] Department of Agricultural and Environmental Sciences (DiSAA), University of Milan, Via Celoria 2, 20133 Milan, Italy; emanuele.morlotti@unimi.it (E.M.); bischetti@unimi.it (G.B.B.)
[2] Centre of Applied Studies for the Sustainable Management and Protection of Mountain Areas (Ge.S.Di.Mont), University of Milan, Via Morino 8, Edolo, 25048 Brescia, Italy
[3] Earth Observation Center—Environmental Protection Agency of Lombardy (ARPA), 20124 Milan, Italy; v.sacchetti@arpalombardia.it (V.G.S.); d.bellingeri@arpalombardia.it (D.B.)
* Correspondence: alessio.cislaghi@unimi.it; Tel.: +39-02-503-16903

Abstract: Sediment management is fundamental for managing mountain watercourses and their upslope catchment. A multidisciplinary approach—not limited to the discipline of hydraulics—is necessary for investigating the alterations in sediment transport along the watercourse by detecting those reaches dominated by erosion and deposition processes, by quantifying the sediment volume change, by assessing the functionality of the existing torrent control structures, and by delimitating the riparian vegetation patches. To pursue these goals, specific continuous monitoring is essential, despite being extremely rare in mountain catchments. The present study proposed an integrated approach to determine the hydro-morphological–sedimentological–ecological state of a mountain watercourse though field- and desk-based analyses. Such an integral approach includes a rainfall–runoff model, a morphological change analysis and the application of empirical formulations for estimating peak discharge, mobilizable sediment/large wood volume and watercourse hydraulic capacity, at reach and catchment scales. The procedure was tested on the Upper Adda River catchment (North Italy). The results identified where and with what priority maintenance and monitoring activities must be carried out, considering sediment regime, torrent control structures and vegetation. This study is an example of how it is possible to enhance all existing information through successive qualitative and quantitative approximations and to concentrate new resources (human and economic) on specific gaps, for drafting a scientifically robust and practical sediment management plan.

Keywords: watercourse; torrent dynamics; flood; risk management; aggradation; riparian vegetation; torrent control structures; sediment budget; rainfall–runoff model

Citation: Cislaghi, A.; Morlotti, E.; Sacchetti, V.G.; Bellingeri, D.; Bischetti, G.B. Towards a Modern and Sustainable Sediment Management Plan in Mountain Catchment. *GeoHazards* **2024**, *5*, 1125–1151. https://doi.org/10.3390/geohazards5040053

Academic Editor: Kevin Schmidt

Received: 22 August 2024
Revised: 13 October 2024
Accepted: 16 October 2024
Published: 17 October 2024

1. Introduction

Sediments represent the most important element in the dynamics of mountain streams. They determine all the physical processes associated with their mobility, and influence water level, channel evolution, habitat changes and landscape value [1]. Moreover, mountain catchments are the first landscape elements that are facing an epochal challenge. In particular, the European Alpine space is a vulnerable ecosystem that is extremely exposed to climate change, due to the climate amplification of the dynamics of high-altitude snow cover, albedo, and heat budget [2]. Measuring from the late 19th century onward, the average temperature over the Alps has risen approximately 2 °C between 1880 and 2010, two times more than the global warning [3,4]. This rate of warming is affecting seasonal weather patterns, glacier retreat, permafrost thawing, and snow cover persistence, leading to an acceleration in the sedimentological and hydrological regime changes in mountains ecosystems [5]. At high altitudes, sources of sediments increase the production of huge amounts of materials, exacerbated by the increase in intense rainfall frequency [6], by the

past excessive artificial modification of the watercourse [7], and by the abandonment of the territory (i.e., the daily monitoring and maintenance of the mountain catchment) [8]. The consequences, in practice, can vary significantly, from the streambed incision involving streambanks' failure and a straightening watercourse [9–11], to the streambed aggradation that increases the flood hazard for the surrounding areas [12]. Despite this evidence, quantifying the sediment flux (especially the bedload rate) is extremely complex and depends on the intrinsic local features of the mountain catchments [13–17].

For this reason, sediment management (SM)—which represents one of the human strategies for conserving, preserving, and restoring the river environment, and for undertaking countermeasures to mitigate the flood risk—remains an arduous challenge. SM attracts more stakeholders, such as (i) regional and local authorities that control waterways, torrent control structures, the mining of materials, fisheries, etc.; (ii) researchers that investigate the torrent dynamics over the time; (iii) sediment miners that legally exploit the economy of the sediment as building materials; (iv) the policy makers that must regulate and comply with regulations of supranational organizations; and (v) the citizens that who live or own private properties in proximity of the watercourse. Despite or precisely because of this, SM is generally fragmented [18] and is rarely based upon scientific knowledge [19]. In this context, SM must be an essential human activity focused on controlling the entire sediment cycle at catchment scale and not only a unit of sediment at a time, and must integrate various different goals to be more shared and maintainable as possible [20]. Thus, a different approach is desirable and must begin from drafting a modern and sustainable sediment management plan (SMP), incorporating knowledge (past and present), scientific advances (prediction), multidisciplinary actions, and the ability to propose different scenarios of intervention at catchment scale. In addition, SMP avoids the error of focusing on the hydraulic aspect, favoring the construction of transverse and longitudinal torrent control structures and the massive extraction of sediment from the streambed [20,21], worsening the morphological quality [22]. Thus, the present study aims to propose a generalizable procedure for identifying and prioritizing ordinary and extraordinary maintenance interventions through the scientific investigation of the elements constituting the watercourse (sediment, vegetation, streamflow and existing torrent control structures) and through leveraging the set of information and analyses already present in the databases of local, regional, and national authorities. Such an approach would have the advantage of reducing the time of the technical decision-making process, allocating funds to address specific deficiencies in the diagnostic framework, conducting additional monitoring activities, and/or increasing the necessary interventions.

2. Materials and Methods

2.1. Case Study

The case study is approximately 12 km of the Adda River (Figure 1) flowing north to south, from the municipality of Bormio to the village of Le Prese in Sondalo, located in the Upper Valtellina (Lombardy, North Italy). The enclosing perimeter of the surveyed watercourse encompasses a catchment of about 563 km^2 with a range of altitude from 946 to 3829 m asl. The catchment area is predominantly covered by periglacial landforms (41%) with scarce presence of vegetation, forests (22%) and pasture (13%), while urbanized areas (1%) are concentrated along the main watercourse. The forests are mainly conifers, detailed as follows: Norway spruce (34%) and European larch (40%) are the dominant species, whereas mountain pine (17%) is the secondary species. The glaciers and perennial snowpack covered approximately 21.6 km^2, concentrated in the Forni glacier in the western part. The lithology of the study area is homogeneous, with Leptosols and Podzols over the hillslopes, and Cambisols along the valley bottom.

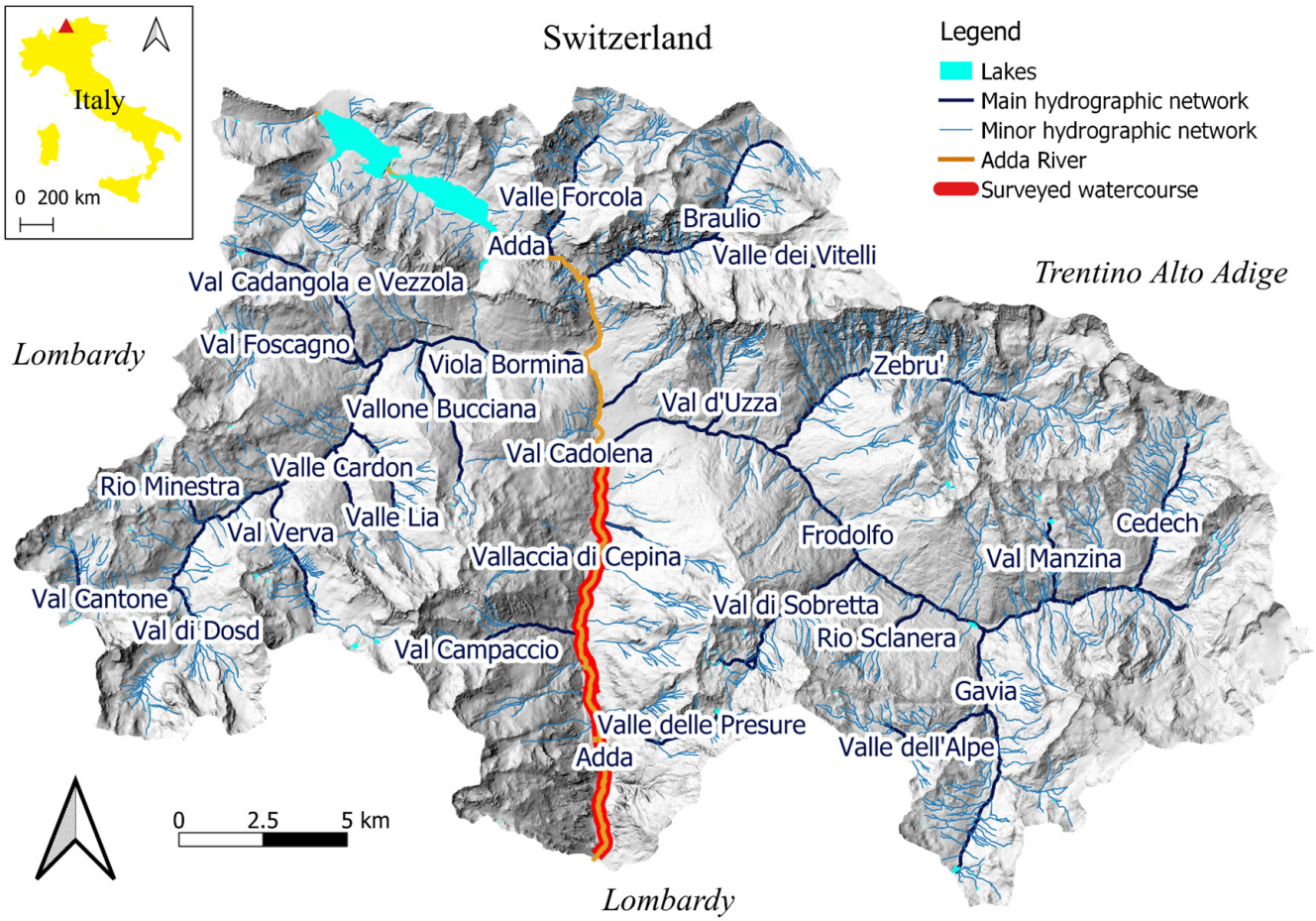

Figure 1. Location of the surveyed 12 km of Adda River flowing north to south, in the Upper Valtellina (Lombardy, North Italy).

Concerning the watercourse, the Adda River shows a torrential regime that exacerbates the flood and debris flood events. To mitigate the potential damages caused by these hydro-sedimentological processes, flood protections were built along the watercourse, including longitudinal structures to reinforce the streambank and raise the levees, and a transverse torrent control structure to reduce the longitudinal streambed slope and, as a consequence, the sediment transport. In addition, the local authorities ordered emergency interventions to reduce the streambed aggradation of the watercourse, and listed them in a specific dataset including information on location, date, extracted/removed sediment volume, costs, etc. The case study was extensively investigated from several points of view using many technical maps at the following detailed scales: geological map (1:10,000), soil map (1:50,000), land use map (1:10,000), forestry map (1:10,000), an inventory of landslide events (date, polygon, etc.), and a time series of Digital Elevation Models (DEMs) surveyed in 2008, 2014, and 2022.

2.2. Hydro–Geo-Morphological, Sedimentological and Ecological Integrated Analysis

Hydro–geo-morphological, sedimentological and ecological integrated analysis (HySEcA, hereafter) is the proposed methodology for providing an overall characterization of the watercourse and its catchment, based on the assessment of the hydrological and sedimentological processes occurring on the hillslopes and along the river network. HySEcA is subdivided into the following three phases (Figure 2): (i) the segmentation of river network and the delineation of the tributaries and subcatchments, (ii) the completion of the available data through specific activities of field campaign, and (iii) the application of qualitative and quantitative approaches to estimate the watercourse dynamics and the

magnitude of ordinary and extreme events that can potentially occur, associated with the sediment transport into the river network.

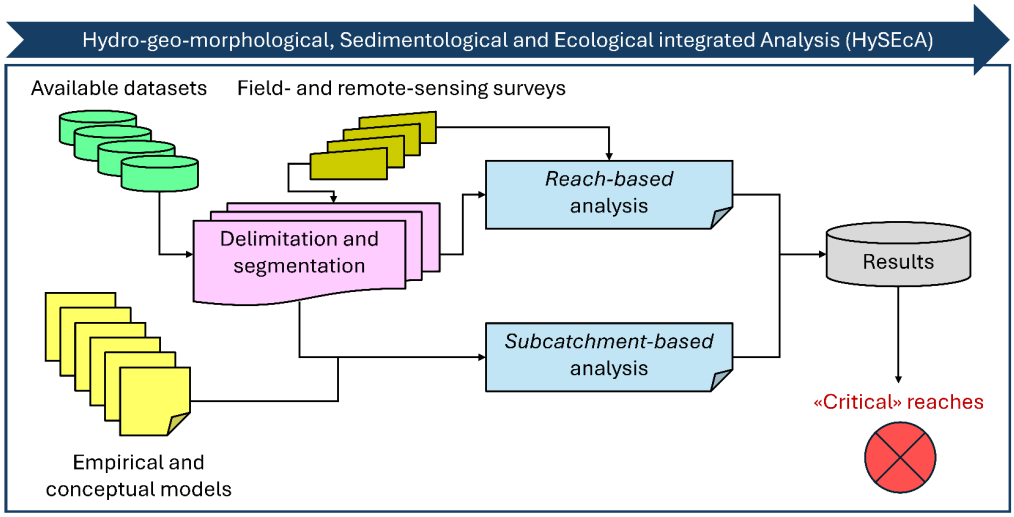

Figure 2. Framework of the hydro–geo-morphological, sedimentological and ecological integrated analysis (HySEcA), on which basis operational and monitoring measures are proposed in the sediment management plan.

2.2.1. Delimitation of Reaches and Subcatchments

The delimitation of reaches is based on an expert judgment on the fluvial dynamics that lead to the adjustments of the channel form, and follows the procedure of the Morphological Quality Index proposed by Rinaldi et al. (2013, 2015) [23,24]. The first phase consisted of subdividing the watercourse into relatively homogeneous reaches, delimited by boundary conditions. Key factors commonly investigated to identify the homogeneous spatial units include the absence of significant changes in valley setting and in channel slope, as well as the lack of substantial flow and sediment loads. Alternatively, all the confluences with the tributaries and the sudden changes in geological and geomorphological characteristics of the watercourse can be detected as boundaries of homogeneous reaches. More details are given in Brierley and Fryirs (2013) [25]. The delimitation in subcatchments is a part of the terrain analysis in Geographical Information System (GIS) research [26,27] and is obtained by an accurate mapping of the river network and the alluvial fans. The river network is a fundamental element of the mountain landscape that can significantly improve the quality of hydrological and sedimentological modeling [28], because its characteristics affect sediment storage, sediment connectivity, sediment flux, and flow velocities [29,30]. The river network starts in source cells called channel heads, which is the upstream-most point of concentrated water flow and sediment transport between definable streambanks [31], with a longitudinally continuous channel downstream. The identification of the channel heads can be carried out (i) directly in the field (excessively time-consuming), (ii) through a geostatistical-based terrain analysis, and (iii) with remote sensing-derived approach [32–34]. From a geomorphological point of view, the river network begins where a threshold of the drainage area (A_s in m^2) is exceeded. In the present study, A_s was calculated for all the cell of DEM according to the longitudinal streambed slope [35–37] and within the range between 500 and 4000 m^2 [38], as follows:

$$A_s(x) = A_0 \cdot s(x)^{\alpha} \quad (1)$$

where s (in m m^{-1}) is the slope of the generic cell (x), whereas A_0 (in m^2) and α (-) are constant values. In the present study, they were set to 1000 m^2 and 2, respectively.

On the other hand, alluvial fans could be recognized as conspicuous sediment deposits transported by upstream tributaries from a mountainous drainage basin [39]. Typically, they assume a semi-conical shape with a fan apex, located at the change in slope from the

mountain catchment to a contiguous valley or alluvial plain. These points were considered as the outlet of the subcatchment [40,41]. Both the procedures include a topographical analysis on the DEM using a set of topographic and hydrological functions, implemented into the library *TopoToolbox* for the software MATLAB (R2023b) [42].

2.2.2. Data Collection

The second phase consisted of filling or updating the database integrating with (i) high-resolution DEM derived by Structure-from-Motion (SfM) techniques processing Unmanned Aerial System (UAS) images or Light Detection and Ranging (LiDAR) point clouds; (ii) the in-channel grain size distribution; and (iii) the identification and classification of vegetation communities in riparian zone.

2.2.3. Subcatchment-Based Analysis

The subcatchment-based analysis is part of the third phase of HySEcA, aiming to assess the magnitude of peak discharge, and the sediment/large wood volume mobilized by surface erosion and debris flow, associated with ordinary or extreme events.

Design Peak Discharge

The peak runoff in ungauged subcatchment areas was established through a rainfall–runoff model [43,44]. This quantitative analysis includes the prediction of an effective hyetograph and of the flood hydrograph, and is composed by several steps.

- Calculating of the total precipitation (P in mm) using the Intensity–Duration–Frequency (IDF) curves provided by the Environmental Protection Agency of Lombardy (ARPA; https://idro.arpalombardia.it/). A common approach to express IDF curves for the high-altitude areas where the contribution of snowpack melting is significant [45,46] is as a power law:

$$P(dr, RP) = a_1 \cdot w_1 \cdot dr^n \tag{2}$$

where a_1, w_1 and n (-) are the parameters of the power law estimated locally, RP is the return period (in years), and dr is the precipitation duration (in hours). The parameter w_1 (-) represents the generalized extreme value (GEV) with the following formula:

$$w_1 = \varepsilon + \frac{\alpha}{\kappa} \cdot \left\{ 1 - \left[\ln\left(\frac{RP}{RP - 1} \right) \right]^{\kappa} \right\} \tag{3}$$

where ε, α and κ (-) are the parameters of GEV distribution. Seven different return periods were considered (i.e., 2, 10, 30, 50, 100, 200, 500 years).

- Calculating the rainfall excess (Q in mm) using the Soil Conservation Service Curve Number (SCS-CN) method [47–49]. SCS-CN is based on the water balance equation and calculated the direct runoff (in mm) as follows:

$$Q = \frac{(P - \lambda \cdot S)^2}{(P - \lambda \cdot S) + S}, \; P > \lambda \cdot S \tag{4}$$

where S is the potential maximum retention or infiltration (in mm), and λ (-) is the initial abstraction coefficient. In this case, λ assumes an original value of 0.2; however, some studies verified that for small catchments, its value is considerably lower [50,51]. In this case, λ was set equal to 0.1.

$$S = 25.4 \cdot \left(\frac{1000}{CN} - 10 \right) \tag{5}$$

where CN (-) is a dimensionless number ranging from 0 to 100. The CN parameter was estimated over the overall subcatchment according to several features such as hydrologic

soil group, land cover type, hydrologic condition, and antecedent runoff condition [52–54], as reported in Supplementary Materials A.

- Designing the effective hyetograph through the distribution of the rainfall excess, i.e., the effective precipitation depth is temporally spatially distributed using Huff's hyetograph shape [55].
- Designing the flood hydrograph (i.e., the rainfall excess was transformed into surface runoff until the outlet cross-section) and modeling the hydrological propagation within the catchment. This step consisted of the application of WFIUH-1par, a combined approach between the instantaneous unit hydrograph (IUH) concept and the width function (WF) [56]. This model predicted the travel time distribution using a single parameter, i.e., the flow velocity, over the time (t) as follows:

$$WFIUH(t) = \frac{l_c(x)}{v_c(x)} + \frac{l_h(x)}{v_h(x)} \quad (6)$$

where l_c and l_h (in m) are the channel and hillslope flow path for the generic cell (x) among the raster of catchment, and v_c and v_h (in m s^{-1}) are the channel and hillslope flow velocities in the single cell x. The channel velocity is empirically estimated according to the catchment area (A in km^2) [57–61], as follows:

$$v_c(x) = 0.33 \cdot A(x)^{0.12} \quad (7)$$

Conversely, the hillslope velocities were defined using spatially distributed empirical formulas based on hillslope inclination and land use information extrapolated from digital topographic data, as follows:

$$v_h(x) = k_u \cdot s(x)^{0.5} \quad (8)$$

where k_u (-) is a coefficient related to soil use [62,63]. The resulting velocities were restricted within the 0.02–2 m s^{-1} range to avoid unrealistic values, as suggested by Grimaldi et al. (2010) [64]. The values of k_u parameter according to land cover are available in the Supplementary Materials B.

Sediment and Large Wood Mobilizable Budget

The assessment of sediment volume mobilized by debris flows is generally obtained using empirical formulations [65–69]. Among the wide spectrum of experience, a recent statistical analysis was conducted on a 537 debris flow event which occurred in the Italian Northeastern Alps and developed a linear regression between A and debris flow volumes (Gs in m^3) [70], as follows:

$$Gs_{50\%} = (2620 \pm 60) \cdot A^{0.67 \pm 0.02} \quad (9)$$

$$Gs_{99\%} = (77000 \pm 7000) \cdot A^{1.01 \pm 0.06} \quad (10)$$

Equation (9) provides the magnitude of an ordinary event, whereas Equation (10) represents an envelope curve that predicted very large volumes up to approximately 10 Mm^3 for the largest drainage areas, often responsible for severe damage.

The estimation of average annual sediment volume produced by surface erosion processes (G in m^3 year^{-1}) was obtained by a modified version of an Erosion Potential Model (EPM), originally developed by Gavrilović (1959) [71], and modified by Milanesi et al. (2016) [72] for the Alpine region. The model is based on the relationship between G and several factors describing the main features of the catchments as follows:

$$G = T \cdot h \cdot \pi \cdot Z^{1.5} \cdot A \cdot B \quad (11)$$

where T (-) is the temperature coefficient, h (in mm) is the mean annual cumulative rainfall, π (-) is the mathematical constant equal to 3.14, Z (-) represents the potential erosivity

coefficient, whereas B (-) is the percentage of sediments that reaches the outlet. The parameter T is defined as follows:

$$T = \left(\frac{t_m}{10} + 0.1\right)^{0.5} \tag{12}$$

where t_m is the mean annual temperature (in °C). In a cold climate, this value is calculated only for the sediment yield period excluding the winter [72].

The parameter Z is defined as

$$Z = X \cdot Y \cdot \left(\phi + S_b^{0.5}\right) \tag{13}$$

where X (-) describes the protection against the erosion processes given by the land cover, Y (-) is the soil resistance against the surface runoff, ϕ (-) indicates the intensity of the active erosion processes, and S_b is the mean slope of the catchment (in m m^{-1}). The values of the parameters X, Y and ϕ are reported in Supplementary Materials C.

The parameter B is defined as

$$B = \min\left[\frac{4 \cdot (O \cdot D)^{0.5}}{L_c + 10};\ \frac{L \cdot (O \cdot D)^{0.5}}{(L_c + 10) \cdot A}\right] \tag{14}$$

where O (in km) is the perimeter of the catchment, D (in km) is the mean geodetic relief, L_c (in km) is the linear dimension of the catchment along the main channel, and L (in km) is the longest hydrological path.

Furthermore, the estimation of the potential maximum large wood volume, recruited during an extreme event, was provided by an envelope curve based on dataset collected in Switzerland, France and Italy [73]. The formula is

$$V_{LW} = 1170 \cdot A^{0.4} \tag{15}$$

where V_{LW} (in m^3) represents the specific large wood volume (solid, no pores) transported during a flood.

Sediment Connectivity Analysis

Quantifying the mobilizable sediment is only a relative part of the complex process that also includes sediment redistribution and movement [74]. Thus, it is necessary to introduce the concept of sediment connectivity, which is the degree of linkage controlling sediment fluxes throughout the landscape, describing the physical transfer from a source to a sink [75–79]. An indicator useful to estimate this catchment predisposition is the index of connectivity (IC), developed by Borselli et al. (2008) [80] and further adjusted by Cavalli et al. (2013) [81]. IC (-) is the logarithm of the ratio between an upslope and a downslope component expressing the potential for the downward routing of the sediment-produced upslope and the sediment flux path length to the nearest sink along a flow line, respectively, for each grid cell (x) of a catchment, expressed as follows:

$$IC(x) = \log_{10}\left(\frac{\overline{W}(x) \cdot \bar{s}(x) \cdot \sqrt{a(x)}}{\sum_i \frac{d(x)}{W(x) \cdot s(x)}}\right) \tag{16}$$

where x is the generic cell of the raster, a (in m^2) is the upslope area, d (in m) is the length of the steepest flow line between the grid cell (x) and the target area, s (in m m^{-1}) is the slope of the steepest flow in the grid cell (x) and W (-) is the weighting factor computed from the standard deviation of the residual topography, i.e., the difference between the point elevation and the mean average taken on a moving square window of a side measuring

5 pixels. Note that $\overline{W}$ and $\bar{s}$ are the average weighting factor for the average slope gradient of the upslope contributing area with respect to the generic cell (x).

2.2.4. Reach-Based Analysis

The reach-based analysis included (i) the measurements of volumetric variations within the streambed through the calculation of the Difference of DEMs over time (DoDs), (ii) the assessment of functionality/performance of the existing transverse torrent control structures, and (iii) the detection and classification of riparian vegetation patches.

Sediment Volume Change

The main output of the reach-based analysis was the sediment volume change along the watercourse. The sediment volume change was obtained by summing the time series of DoDs. The DEMs were collected into a dataset including details on survey accuracy, sampling strategy, topographic roughness, and interpolation procedure that can strongly influence the measurement errors [82–85]. Using such data, DoDs were calculated though different procedures [86–88]. The first and simplest approach (M.0) was the calculation of DoD by subtracting raw successive DEMs without correction. The second procedure (M.1) consisted of summing the raw volumetric change exclusively upon a critical threshold error U_c (in mm), also called Level of Detection, which was fixed equal to the 84th percentile of grain size distribution d_{84} (in mm). The last alternative methodology (M.2) expressed the critical threshold as follows:

$$U_c = \delta \cdot \sqrt{SDE_1 + SDE_2} \tag{17}$$

where SDE (in mm^2) is the standard deviation of the errors (differences) between the elevation of the Ground Control Points (GCPs) and those of the reconstructed DEM, whereas the subscripts (1 and 2) indicate the two successive raw DEMs. The parameter δ (-) represents the critical t-distribution values at the selected confidence level, under the assumption that the errors follow a normal distribution. In the present case, the confidence limit was 95% and the $\delta \geq 1.96$ [89]. To apply the procedure M1, a campaign of granulometric surveys was conducted using the traditional methodology of Wolman Pebble counting [90,91] for each reach.

Monitoring Torrent Control Structures

The torrent control structures play a significant role in controlling sediment transport [92]. Monitoring their functionality is essential and can be exclusively conducted through the first-level inspections, as described in Cislaghi et al. (2024) [93]. The first-level inspection is a meticulous scrutiny of the overall structure that allows us to assess the performance or, better, the loss of functionality, of the existing torrent control structures using a qualitative indicator. This metric is the Loss of Functionality Index (*LoFI*), ranging from 1 low (unaltered functionality) to 4 high (no residual functionality). The causes of deteriorated functionality can be detailed as (i) sediment deposition that can modify the streamflow concentration and can alter energy dissipation; (ii) the deposition of coarse or large wood materials that can obstruct the cross-section or can deviate the streamflow only on a side of the channel; (iii) erosion of the foundations or a specific side of the torrent control structures; and (iv) the uncontrolled colonization of riparian vegetation around and over the structure that can increase flow resistance, hydraulic roughness, and hydraulic depth, as well as reducing hydraulic velocity and impeding the adjusted (or "designed") direction of streamflow. In the present study, the inspectors focused on the first case, assessing the *LoFI* according to the obstruction due to the sediment deposition (Figure 3).

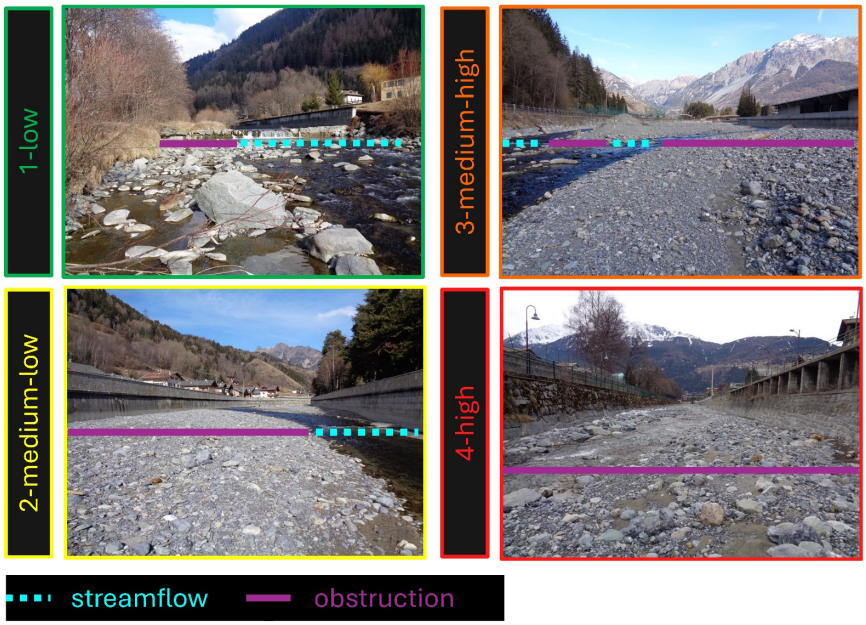

Figure 3. Photographs of transverse torrent control structures that show the four conditions of the Loss of Functionality Index (*LoFI*) according to the percentage of spillway occupied by the sediment. Value 1, or Low, indicates a spillway covered for less than 50%; Value 2, or Medium-low, indicates a coverage between 50 and 75%; Value 3, or Medium-high, indicates a coverage between 75 and 90%; and Value 4, or High, indicates a coverage more than 90%.

Monitoring Riparian Vegetation

Monitoring the vegetation dynamics of the riparian and in-channel colonization is extremely important. The procedure consisted of observing and mapping the riparian vegetation patches over bars, islands, and banks, identifying the dominant species, and identifying their forest management approach, as conducted by Fogliata et al. (2021) [94]. Then, the riparian vegetation community was classified according to its density (negligible, low, medium, or high), as shown in Figure 4.

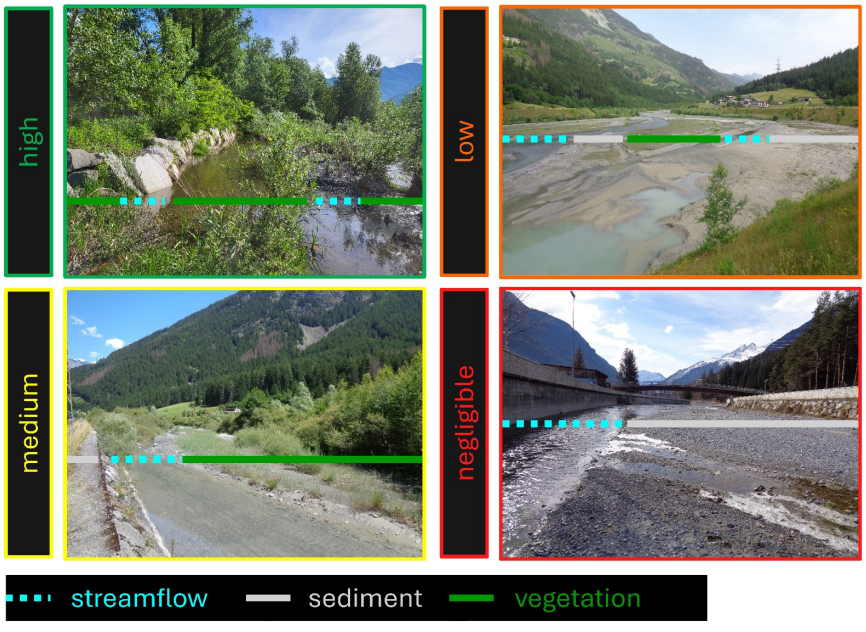

Figure 4. Photographs of riparian vegetation according to colonization density (negligible, low, medium and high).

3. Results

3.1. Delimitation of Reaches and Subcatchments

The first phase of HySEcA distinguished 14 reaches of the surveyed watercourse and 28 subcatchments (Figure 5). These reaches had a length (L_c) of 0.855 km ± 0.586 km with a streambed slope (S_c) of 0.017 m m^{-1} ± 0.020 m m^{-1}. The channel slope is strongly influenced by the presence of more than 50 transverse torrent control structures, approximately 1 every 250 m. The bankfull width (W_c) along the watercourse was 45.52 m on average, varying from 26.71 m to 84.88 m. Table 1 summarizes the hydraulic characteristics of each reach along the watercourse. The subcatchments were delineated considering a minimum threshold area of 0.1 km^2. Their area was 2.35 km^2 ± 2.06 km^2 and ranged from 0.11 km^2 (8A_2) to 9.76 km^2 (5D_1). The confluences with the tributaries were located at an altitude ranging from 952 m asl (8A_7) and 1163 m asl (4A_1), from downstream to upstream, respectively. The subcatchments had a wide range of hillslope inclination from 0.339 to 0.781 m m^{-1}. This discrepancy was obviously influenced by the topography and was evaluated using the Melton Ratio (MR) [95], i.e., the ration between the basin relief and the square root of the basin area. MR varied from 0.73 (4A_1) to 2.76 (8A_2). Table 2 reports the hydrographic and topographic features of the delineated sub-catchments.

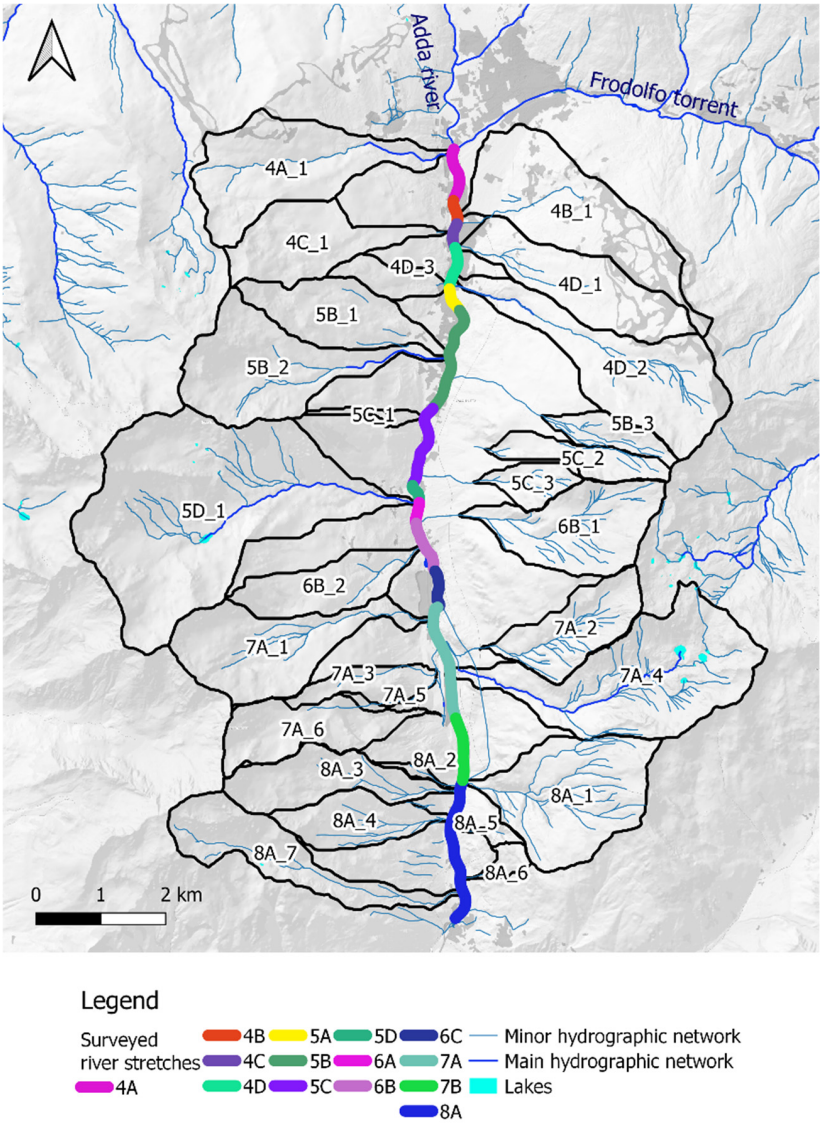

Figure 5. The identification of 14 reaches (from 4A to 8A) and 28 subcatchments (from 4A_1 to 8A_7) for the study area.

Table 1. The hydraulic features of the homogeneous reaches: L_c (in km) is the length of the reach, S_c (in m m^{-1}) is the streambed slope, W_c (in m) is the mean bankfull width, and the presence of crossing infrastructures.

Reach	L_c (km)	S_c (m m^{-1})	W_c (m)	N. of Bridges
4A	0.796	0.013	40.32	1
4B	0.300	0.011	28.64	1
4C	0.382	0.010	41.00	1
4D	0.600	0.009	62.46	1
5A	0.341	0.020	26.71	0
5B	1.691	0.013	27.22	1
5C	1.235	0.009	31.10	1
5D	0.291	0.020	30.00	0
6A	0.334	0.029	46.38	0
6B	0.742	0.004	70.08	0
6C	0.591	0.002	84.88	0
7A	1.623	0.004	36.92	0
7B	0.972	0.080	63.63	1
8A	2.084	0.021	47.93	1

Table 2. The topographic features of the delineated subcatchments (including toponymy): A (in km^2) is the subcatchment area, L (in km) is the longest past along the river network, Z_{min} (in m) is the minimum elevation inside the subcatchment, Z_{mean} (in m) is the mean elevation inside the subcatchment, Z_{max} (in m) is the maximum elevation inside the subcatchment, S_b (in m m^{-1}) is the mean slope within the subcatchment, L_c (in km) is the length of the main watercourse of the subcatchment, S_c (in m m^{-1}) is the slope of the main watercourse, and MR (km km^{-1}) is the Melton Ratio.

Subcatch.	Toponymy	A (km^2)	L (km)	Z_{min} (m)	Z_{mean} (m)	Z_{max} (m)	S_b (m m^{-1})	L_c (m)	S_c (m m^{-1})	MR (km km^{-1})
4A_1	Cadolena	3.80	4.85	1163	1999	2589	0.394	3.61	0.228	0.73
4B_1	Ciucco	4.21	4.55	1150	1625	2674	0.339	1.78	0.234	0.74
4C_1	Presurina	2.36	3.98	1150	2070	2761	0.427	1.91	0.302	1.05
4D_1	Cagnola	2.81	4.25	1146	1827	2659	0.396	2.01	0.295	0.90
4D_2	Vallecetta	4.09	5.39	1144	2302	3138	0.492	4.39	0.316	0.99
4D_3	Valle del Prete	0.71	2.25	1144	1535	1979	0.433	0.82	0.238	0.99
5B_1	Valcepina	2.23	4.14	1126	1900	2746	0.509	2.70	0.349	1.08
5B_2	Vallaccia	3.65	4.82	1126	2373	3020	0.518	3.62	0.352	0.99
5B_3	Rez de la Piscia	0.99	3.87	1229	2375	3145	0.540	3.06	0.421	1.93
5C_1	Valle Soena	0.23	2.00	1120	1628	2358	0.589	0.82	0.505	2.59
5C_2	Resole	1.09	3.17	1492	2396	3154	0.582	2.32	0.443	1.59
5C_3	Val del Solco	0.72	2.30	1222	2046	2677	0.703	1.73	0.515	1.71
5D_1	Massaniga	9.76	6.41	1106	2469	3414	0.559	5.03	0.274	0.74
6B_1	Novalena	2.96	4.51	1085	2394	3141	0.567	3.40	0.405	1.19
6B_2	Pra Bonelli	1.81	3.84	1082	1820	2640	0.478	0.94	0.331	1.16
7A_1	Vendrello	3.29	4.57	1080	2272	2998	0.535	3.15	0.351	1.06
7A_2	Val Mala	2.02	3.18	1306	2284	2999	0.679	2.05	0.442	1.19
7A_3	Valle Asciutta	0.94	2.99	1102	1698	2528	0.604	0.77	0.471	1.47
7A_4	Presure	5.48	6.60	1096	2416	3062	0.544	5.07	0.236	0.84
7A_5	Motta	0.16	1.60	1169	1598	2072	0.602	0.79	0.470	2.29
7A_6	Val Pola	2.07	4.12	1141	2288	3048	0.555	2.27	0.430	1.32
8A_1	Valle Fine	3.85	3.63	995	2054	2895	0.628	2.57	0.425	0.97
8A_2	Valle Fiorino	0.11	1.46	1010	1495	1931	0.719	0.84	0.544	2.76
8A_3	Valle Cameraccia	2.06	3.98	987	2187	3099	0.605	1.99	0.455	1.47
8A_4	Val di Sovilla	1.53	2.99	972	1857	2646	0.595	1.63	0.519	1.35
8A_5	Pravadina	0.17	1.29	973	1485	1782	0.781	0.08	0.466	1.97
8A_6	Valle del Tegne	0.27	1.50	957	1536	1843	0.638	0.73	0.546	1.69
8A_7	Valle del Corno	2.55	5.40	952	2347	3136	0.567	4.66	0.328	1.37

3.2. Subcatchment-Based Analysis

The subcatchment-based analysis provided quantitative estimates based on a reliable rainfall–runoff approach and empirical relationships. The rainfall–runoff model requested the estimation of CN parameter that, although the dominant land cover was the forest, ranged from 59 to 80, because of different soil properties (hydrologic soli group and land cover). The rainfall–runoff model assessed the design discharge according to the different return periods (Table 3). On average, the design peak discharge per unit catchment area largely varied from 0.34 m^3 s^{-1} km^{-2} for a 10-year return period to 3.23 m^3 s^{-1} km^{-2} for a 200-year return period. Only one subcatchment revealed a significant larger design discharge per unit of area (7A_5).

Table 3. Curve number (*CN* dimensionless) and design discharge (*Q* in m^3 s^{-1}) for different return periods (*RP* in years).

Subcatchment	*CN* (-)	*Q* (m^3 s^{-1})						
		***RP* = 2**	***RP* = 10**	***RP* = 30**	***RP* = 50**	***RP* = 100**	***RP* = 200**	***RP* = 500**
4A_1	63.85	0.08	1.10	2.63	3.64	5.38	7.58	11.36
4B_1	65.72	0.24	1.75	3.61	4.77	6.72	9.04	12.88
4C_1	66.01	0.33	1.33	2.39	3.00	3.96	5.15	7.08
4D_1	66.29	0.17	1.12	2.29	2.98	4.11	5.55	7.81
4D_2	67.77	0.13	1.75	4.29	6.01	8.89	12.66	18.97
4D_3	63.05	<0.01	<0.01	0.02	0.05	0.33	0.85	2.10
5B_1	63.64	0.03	0.50	1.35	1.99	3.07	4.46	6.91
5B_2	73.95	0.46	2.91	5.95	7.94	10.95	14.78	21.17
5B_3	75.50	<0.01	0.26	1.13	1.76	3.00	4.59	7.28
5C_1	62.88	<0.01	0.04	0.12	0.17	0.28	0.42	0.67
5C_2	72.64	0.01	0.17	0.90	1.51	2.65	4.31	7.19
5C_3	65.42	<0.01	<0.01	0.07	0.26	0.70	1.41	2.68
5D_1	75.30	2.43	11.32	21.33	27.23	37.03	48.85	67.94
6B_1	74.24	0.04	1.42	4.11	6.13	9.56	14.10	22.16
6B_2	64.71	0.08	0.62	1.33	1.76	2.50	3.39	4.87
7A_1	71.42	0.29	2.20	4.55	6.06	8.57	11.65	16.84
7A_2	71.70	0.25	1.81	3.79	5.00	6.99	9.44	13.38
7A_3	65.28	0.05	0.34	0.69	0.91	1.29	1.73	2.49
7A_4	75.42	0.62	4.69	9.95	13.22	18.60	25.50	36.61
7A_5	80.02	<0.01	0.14	0.41	0.60	0.91	1.29	1.91
7A_6	78.99	0.25	1.84	3.96	5.10	7.41	9.84	14.43
8A_1	67.94	0.39	2.60	5.33	6.96	9.65	12.94	18.25
8A_2	66.15	<0.01	0.02	0.07	0.11	0.19	0.29	0.48
8A_3	71.35	0.15	1.11	2.33	3.11	4.38	5.95	8.46
8A_4	63.87	0.04	0.56	1.29	1.77	2.64	3.67	5.42
8A_5	58.70	<0.01	0.02	0.07	0.12	0.21	0.34	0.55
8A_6	61.67	<0.01	0.05	0.16	0.24	0.38	0.57	0.89
8A_7	73.68	0.2	2.05	4.69	6.33	9.12	12.54	18.66

The empirical approaches predicted the potential mobilizable volume of sediment and large wood from the hillslope to the outlet (Table 4). EPM estimated the sediment annual yield from around 50 m^3 $year^{-1}$ for the smallest subcatchments to more than 10,000 m^3 $year^{-1}$ for the largest one (5D_1). Such variability was also evident when weighting the EPM's results on the subcatchment area. The sediment annual yield per unit of area ranged from 62 m^3 km^{-2} $year^{-1}$ (4C_1) to 3168 m^3 km^{-2} $year^{-1}$ (5B_3). The empirical approaches proposed by Marchi et al. (2019) [70] provided potential sediment production from 602 m^3 to 12,058 m^3 for frequent debris flow events (Equation (9)), and from 8384 m^3 to 768,974 m^3 for extreme events (Equation (10)). Moreover, the formula proposed by Comiti et al. (2016) [73] predicted a mobilization of large wood materials ranging from 486 m^3 to 2911 m^3. The results showed that the ratio between large wood and sediment volume ranged from 0.38% to 5.80%. Grouping these results by the reach where the conflu-

ences with the tributaries are located, the downstream reaches 7A and 8A were prone to a high production of sediment and large wood volumes, followed by the reaches 4D, 5B, and 5D in the middle of the surveyed watercourse. Such quantification, however, is not enough to design appropriate countermeasures, since the sediment connectivity plays an important role in sediment transport. In fact, the calculation of *IC* showed how the downstream subcatchments (from 7A to 8A), although the source of the most sediment, had some areas that were disconnected from the sediment compared to the upstream subcatchments (from 4A to 4D).

Table 4. Estimates of sediment yields, potential mobilized sediment and large wood materials from extreme events (debris flow and storm), and sediment connectivity: G is the sediment annual yield (in m^3 $year^{-1}$), G_s is the sediment production by frequent debris flow event (in m^3), V_{lw} is the volume of large wood mobilized by an extreme event (in m^3), IC_{50} and IC_{95} are the median and the 95th percentile of the index of connectivity (-).

Subcatchment	G (m^3 $year^{-1}$)	Gs_{50} (m^3)	Gs_{99} (m^3)	V_{lw} (m^3)	IC_{50} (-)	IC_{95} (-)
4A_1	853	6406	296,363	1995	−1.997	−0.689
4B_1	558	6865	328,940	2079	−2.403	−0.891
4C_1	146	4651	182,913	1648	−2.258	−1.158
4D_1	651	5235	218,619	1769	−2.210	−0.775
4D_3	50	2080	54,388	1020	−2.369	−1.271
4D_2	4631	6734	319,520	2056	−1.900	−0.650
5B_3	2497	2234	60,543	1064	−1.862	−0.601
5B_2	6888	6241	284,921	1964	−1.951	−0.628
5B_1	408	4482	172,981	1612	−2.361	−1.121
5C_2	1721	2771	83,767	1210	−1.857	−0.696
5C_3	341	2062	53,667	1014	−1.436	−0.299
5C_1	92	975	17,356	649	−1.540	−0.243
5D_1	10,745	12,058	768,974	2911	−1.938	−0.746
6B_2	519	3892	139,828	1482	−2.340	−1.135
6B_1	2828	5341	225,307	1790	−1.774	−0.481
7A_1	2138	5814	256,074	1883	−2.057	−0.656
7A_2	1797	4190	156,248	1548	−1.575	−0.309
7A_6	912	4268	160,699	1566	−1.834	−0.515
7A_3	404	2520	72,627	1143	−1.826	−0.730
7A_4	8287	8193	429,411	2311	−1.866	−0.409
7A_5	141	684	10,177	525	−1.712	−0.279
8A_5	73	794	12,742	574	−1.689	−0.320
8A_4	386	3487	118,460	1388	−1.765	−0.540
8A_3	1210	4256	159,988	1563	−1.753	−0.413
8A_7	1784	4900	197,873	1700	−1.667	−0.378
8A_6	46	1101	20,827	697	−1.600	−0.217
8A_1	1967	6466	300,525	2006	−1.619	−0.305
8A_2	180	602	8384	486	−1.259	0.211

3.3. Reach-Based Analysis

The reach-based analysis achieved observations of the hydraulic and morphological dynamics over time. First, the assessment of the sediment change was obtained by calculating the two DoDs to two timespans, 2014–2008 and 2022–2014. The available DEMs (2008, 2014, 2022) were homogenized in terms of spatial resolution. In fact, the resolutions of the DEMs were quite different; the more recent DEM had the highest resolution, around 0.05 m $pixel^{-1}$, whereas the others had a resolution of moderate quality of 0.50 m $pixel^{-1}$. To apply the procedures M.1 and M.2, U_c was estimated; considering d_{84} as the representative diameter, each reach was measured and the errors were calculated on more than 200 GCPs, with 2 for every 100 m of the reach on average. Furthermore, to accurately assess the sediment change, applying the proposed procedure is not enough, since the local authorities arranged for the sediment removal to reduce the risk to the resident population.

Such operations reduced the streambed aggradation and emptied the active channel from deposited materials that caused obstruction for the discharge. Then, the calculated ΔVs were summed to the removed sediment volumes recorded by the local authorities. The spatial distribution of elevation changes revealed a generalized tendency of streambed aggradation, especially along some reaches (Table 5). Over both temporal periods (2022–2008), 10 of the 14 reaches showed a trend towards moderate to significant deposition on the active streambed, and the elevation change ranged from 0.04 m m^{-2} to 2.31 m m^{-2}. Only 4 reaches were exceptions, listed as follows: the reach 5B was probably affected by local extractions (−11,000 m^3 in 2008–2014), whereas the reach 5D revealed a slight tendency to be eroded along the streambed (−1797 m^3 in 2008–2022).

Table 5. The estimation of sediment volume change including the sediment removal (R.0) for each reach among two time-spans (2014–2008 and 2021–2014) according to different procedures (M.0, M.1 and M.2).

Reach	Area (m^2)	d_{84}	U_c (m)		ΔV 2014–2008 (m^3)				ΔV 2021–2014 (m^3)			
		(m)	M.1	M.2	M.0	M.1	M.2	R.0	M.0	M.1	M.2	R.0
4A	53,407	0.064	0.064	0.247	17,485	16,079	11,698	16,000	−17,521	−16,390	−12,731	108,600
4B	11,204	0.072	0.072	0.261	−112	−365	−1081	0	505	452	353	0
4C	17,309	0.055	0.055	0.186	1881	1306	1704	8300	10,915	9803	5308	22,500
4D	40,181	0.041	0.041	0.194	16,557	15,273	12,284	0	7634	6884	4414	10,000
5A	12,134	0.058	0.180	0.129	−2372	−2337	−2277	6000	64	119	167	0
5B	61,197	0.051	0.051	0.124	−12,210	−12,058	−12,084	0	518	1129	929	0
5C	70,051	0.064	0.064	0.224	−1866	−2855	−4893	2500	6422	6441	5654	0
5D	11,657	0.069	0.080	0.131	−1430	−1381	−1325	0	−1182	−867	−472	0
6A	16,274	0.040	0.040	0.276	3598	3472	2828	0	3507	3443	3125	0
6B	110,105	0.032	0.024	0.253	163,960	161,614	149,682	0	73,455	69,192	52,935	0
6C	72,084	0.028	0.028	0.214	66,847	65,415	58,180	0	38,482	36,226	27,414	0
7A	110,836	0.025	0.036	0.195	−3343	−3518	−4428	0	12,025	11,385	9383	0
7B	65,819	0.022	0.022	0.203	14,635	14,166	11,251	0	n.d.	n.d.	n.d.	0
8A	8689	0.044	0.051	0.185	−2271	−2074	−1448	0	n.d.	n.d.	n.d.	0

Second, the reach-based analysis focused on the torrent control structures and their functionality, especially. In the present study, the first-level inspections were conducted on 87 torrent control structures, such as streambank protection, check dams, and submerged sills. These structures were built exclusively with concrete and steel–concrete within the last 30 years. The field observations revealed that approximately 90% showed good or excellent performance ($LoFI$ = 1 or 2). Selecting only the transverse torrent control structures (n = 36), only five indicated a complete loss of functionality ($LoFI$ = 4) due to being inundated by sediment. These structures with deteriorated functionality were in the upper reaches (4A, 4B and 4C), as shown in Figure 6.

Third, the field monitoring observed a low density of riparian vegetation along the entire surveyed watercourse. The in-channel vegetation was almost absent, except for a few more stable bars or islands (Table 6). Along the streambanks, the colonization of the riparian vegetation was more evident. In terms of biodiversity, most of the riparian vegetation was composed of native species, e.g., some species of willows. Only in some reaches (from 6B to 8A) did the butterfly bush (*Buddleja davidii*) colonize the empty space created with deposited sediments or by mitigation interventions.

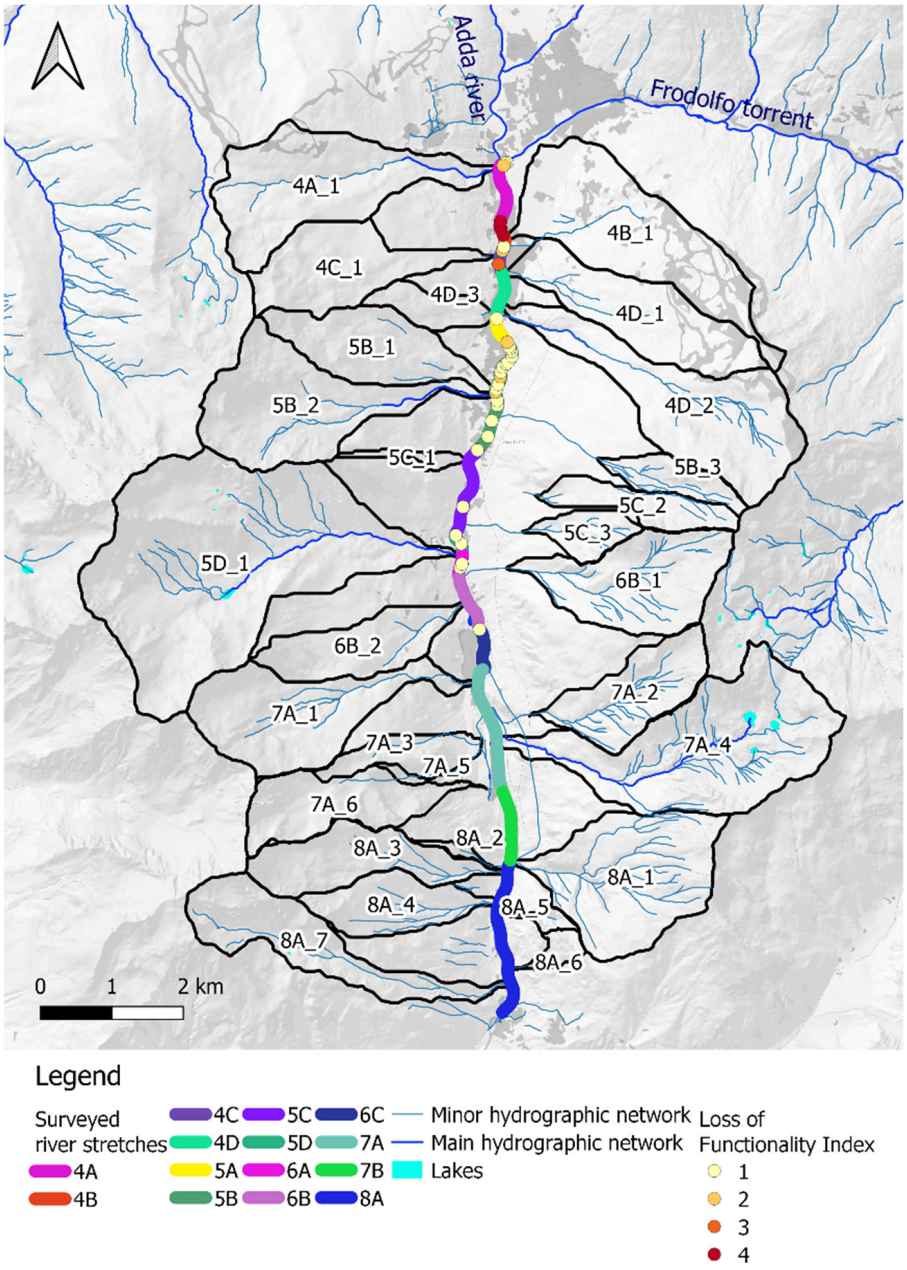

Figure 6. The locations and functionality assessment of the inspected transverse torrent control structures along the surveyed watercourse.

Table 6. Observations provided by monitoring the riparian vegetation along the surveyed watercourse.

Reach	In-Channel	Streambank	Top of Bank	Management	Dominant Species
4A	Negligible	Low	Medium	No management	*Salix purpurea* (purple willow) *Salix alba* (white willow), *Acer pseudoplatanus* (sycamore maple), *Betula pendula* (silver birch), and *Alnus incana* (grey alder)
4B	Negligible	Negligible	Negligible	No management	
4C	Negligible	Negligible	Negligible	No management	
4D	Low	Medium	Medium	Repeated cutting (every year)	*Salix purpurea*, *Salix alba*, and *Salix caprea* (goat willow)

Table 6. *Cont.*

Reach	In-Channel	Streambank	Top of Bank	Management	Dominant Species
5A	Negligible	Low	Medium	No management	*Salix purpurea*, *Salix caprea*, *Fraxinus excelsior* (European ash), *Acer pseudoplatanus*, and *Alnus incana*
5B	Low	Low	Medium	Periodic cutting (3–5 years)	*Salix purpurea*, *Salix alba*, *Alnus incana*, *Sambucus nigra* (elderberry), *Betula pendula*, *Fraxinus excelsior*, *Acer pseudoplatanus*, *Larix* decidua (European larch), *Picea abies* (Norway spruce), and *Populus tremula* (common aspen)
5C	Medium	Medium	Medium	Periodic cutting (3–5 years)	*Alnus incana*, *Salix alba*, *Salix elaeagnos* (rosemary willow), and *Hippopae rhamnoides* (sea buckthorn)
5D	Low	Low	Medium	No management	*Acer pseudoplatanus*, *Picea abies*, *Larix decidua*, *Betula pendula*, *Salix purpurea* and *Fraxinus excelsior*
6A	Low	Low	Medium	No management	*Salix alba*, *Salix purpurea*, *Picea abies*, *Betula pendula*, and *Hippopae rhamnoides*
6B	Low	Low	Medium	No management	*Betula pendula*, *Salix purpurea*, *Salix alba* and *Alnus incana*, *Populus tremula* and *Buddleja davidii* (butterfly bush)
6C	Low	Low	Medium	No management	*Betula pendula* and *Buddleja davidii*
7A	Negligible	Low	Negligible	No management	*Betula pendula*, *Salix elaeagnos* and *Buddleja davidii*
7B	Negligible	Low	Low	No management	*Betula pendula*, *Salix elaeagnos* and *Buddleja davidii*
8A	Low	Low	Medium	No management	*Salix purpurea*, *Alnus incana*, *Buddleja davidii*, *Populus tremula*, and *Pinus sylvestris* (Scots pine)

4. Discussion

4.1. A Diagnostic Approach

The integrated approach of HySEcA can be included in a more general diagnostic approach, drafting the SMP (Figure 7). As proposed by Montgomery and MacDonald (2002) [96], the diagnosis for a watercourse is a careful examination of the hydrological, morphological and sedimentological features, to attempt to understand the river processes and to predict the river dynamics. The diagnosis assesses the channel conditions through the present and past observations, and forecasts the potential future channel condition, through (i) the definition of the system (reaches and subcatchments) and of the drivers influencing the river dynamics; and (ii) the application of models and empirical approaches in terms of qualitative and quantitative outcomes. HySEcA can partially cover the first two steps that can be completed by collecting historical data and by investigating the landscape and the land cover evolution of the surrounding area.

For example, in the present study, the urban development (mainly liked to the touristic sector) and the consequences of climate change strongly influenced the landscape. Indeed, over the last 70 years (1954–2018), there has been a significant increase in urbanization along the main watercourse (+4.5 km^2) and a substantial forest conservation. Conversely, the areas of pastures and agricultural field decreased by more than 10 km^2. Meanwhile, climate change has led to a glacier melting (−31.6 km^2) and a reduction in permafrost areas (difficult to quantify) resulting in an increase in sediment transport. In addition, the catchment area has always been prone to slope instabilities (shallow landslides, rockfalls, and debris flows),

streambank erosion, and significant, dangerous sedimentological–hydrological processes such as debris flood. These areas have been increasing over the time and correspond to approximately 20% of the study case. To contrast this susceptibility, many countermeasures were built to control sediment transport, trapping sediment along the steep tributaries (with more than 450 check dams) and reducing the streambed longitudinal slope along the valley bottom (with more than 200 ground sills). This extensive use of torrent control structures and the delay in designing alternative structures for filtering and dosing sediments, such as the open check dams, indicates a significant limitation of sediment dynamics. In particular, the increase in sediment transport from the proglacial system accelerated the complete filling of sedimentary wedges upstream of each check dam, forcing the movement downstream. Such an amount of sediment, once it reaches the alluvial or colluvial fan, tends to deposit along those reaches where the streambed gradient is relatively low (where there are many ground sills) or where the sediment transport capacity is already saturated. This triggers the streambed aggradation, exacerbating some hydraulic discontinuities, and forcing the local authorities to arrange for the removal of material in the main watercourse, amounting to about 900,000 m^3 from 1997 to 2022, and approximately 250,000 m^3 along the tributaries (Figure 8).

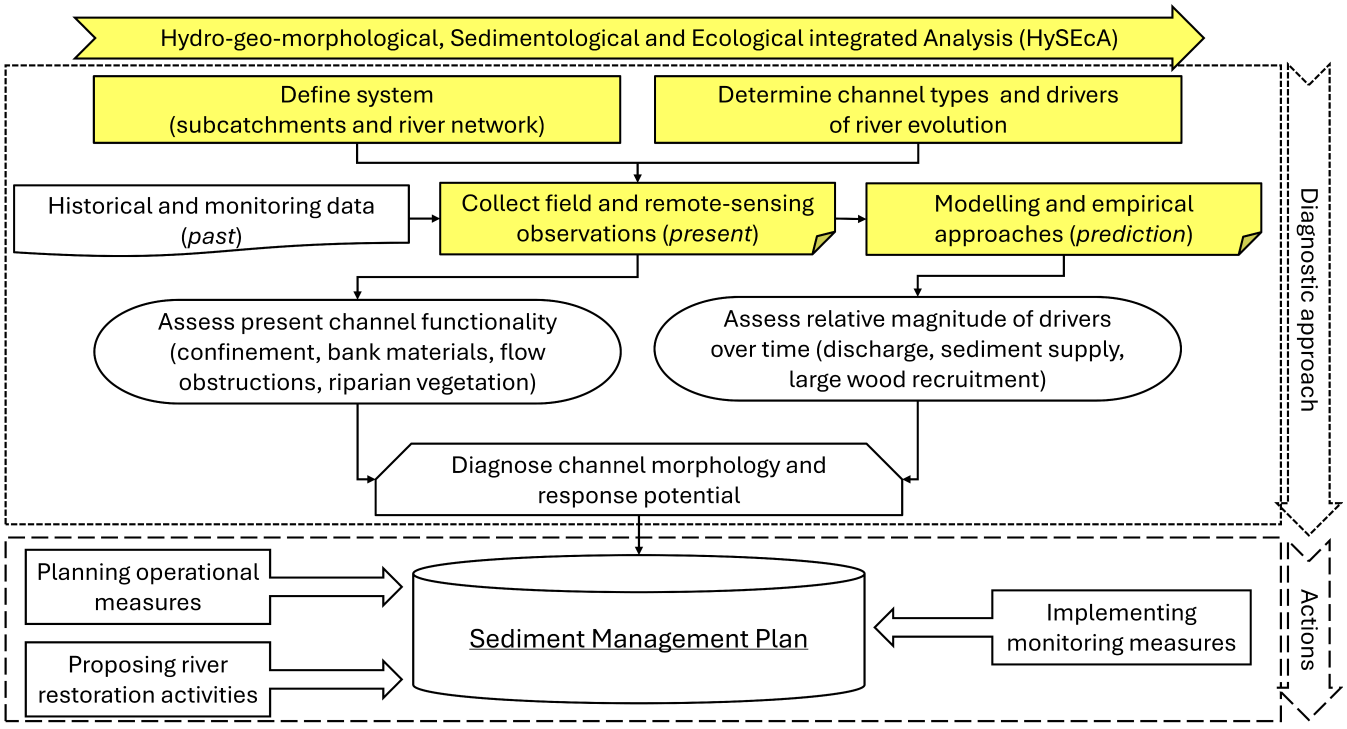

Figure 7. The proposed framework to draft a modern and sustainable sediment management plan.

All these additional observations strongly agreed with the outcomes of the HySEcA procedure. For example, the construction of many retention check dams underlines that the river network of the subcatchments are prone to debris flood and especially to debris flows with a high sediment transport. This evidence was confirmed by examining the catchment predisposition in terms of sediment supply through the simplest method of Wilford et al. (2004) [97], drafting a scattergram using MR and basin length (i.e., the planimetric straight-line length from the fan apex to the most distant point within the subcatchment) with class limits for the hydrogeomorphic processes such as flood, debris flood, and debris flow.

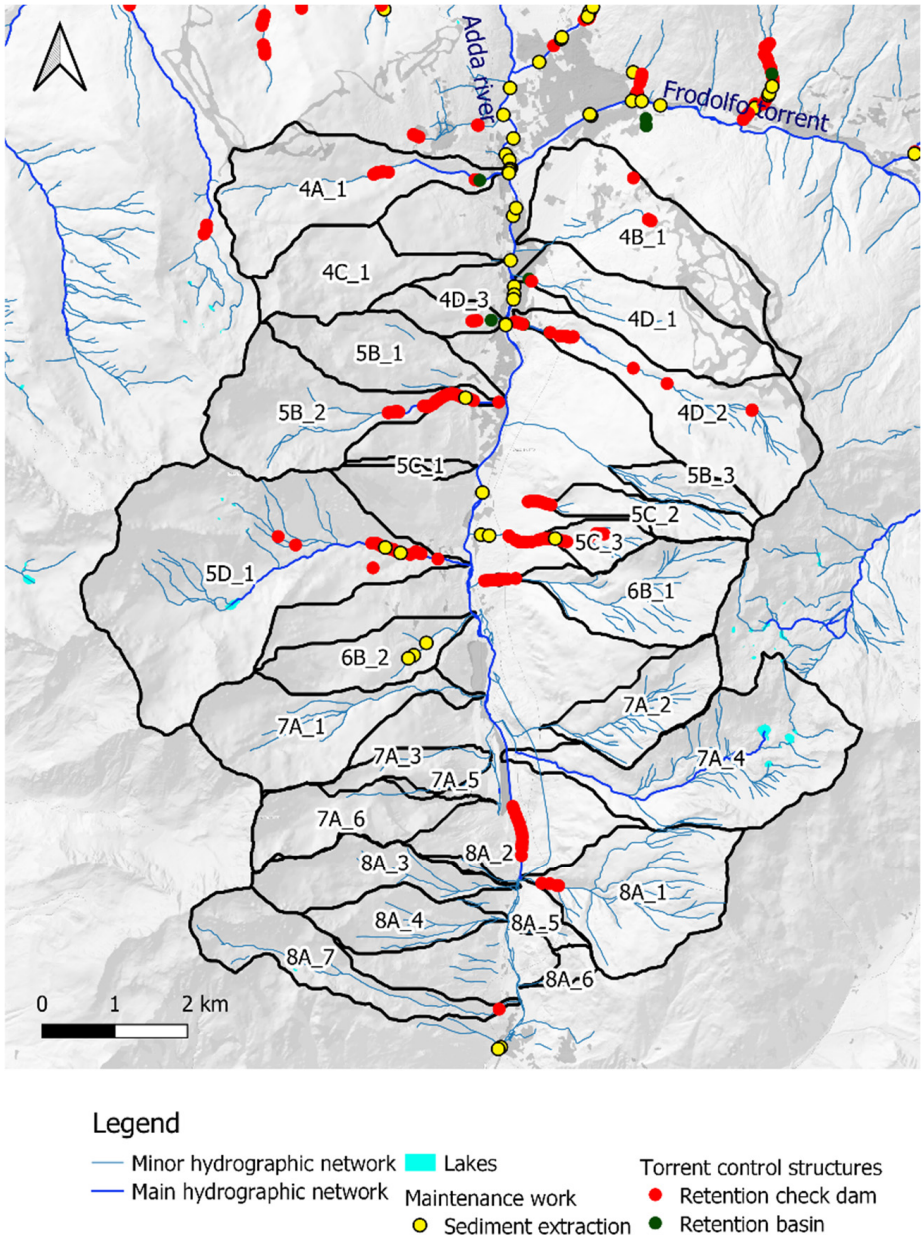

Figure 8. Locations of retention check dams and retention basins in the study area.

Although uncertainties exist, most subcatchments fell into the class of debris flow predisposition, whereas the remaining ones fell into that of debris flood predisposition (Figure 9). In addition, the intrinsic predisposition can be integrated by the degree of sediment connectivity of the subcatchments. In the present study, as expected, the impacts of sediment disconnected areas (i.e., higher values of IC_{50}) were significantly evident for those subcatchments with higher values of MR. The fitted linear regression model confirmed a reasonable relationship ($IC_{50} = 0.396 \cdot MR - 2.399$; $R^2 = 0.430$, p-value < 0.001) as shown in Figure 10. The reach-based analysis completed the diagnostic framework by providing estimates and details on sediment dynamics, torrent control structures, and riparian vegetation. The sediment changes at the reach scale reveal the surplus or the deficit of sediment supply, through quantifying and localizing. The surveys on torrent control structures and riparian vegetation characterized the morphological state of each reach. In the present study, an evident surplus of materials, the presence of transverse torrent control structures completely covered by sediment, and the absence of in-channel riparian vegetation revealed a significant tendency of sediment production and further deposition

within the channel, and a limited transport capacity of the mountain river. Finally, the diagnostic framework also highlighted data gaps, as follows: (i) an updated delimitation and evaluation of the Morphological Quality Index for the homogeneous reaches of the watercourse (in the present study, all the reaches were evaluated in poor morphological condition); (ii) surveys on the in-channel granulometry, essential for predicting the magnitude of sediment transport and for designing appropriate countermeasures; and (iii) a periodic measure of topography (i.e., DEMs) for estimating the volume changes and a potential trend.

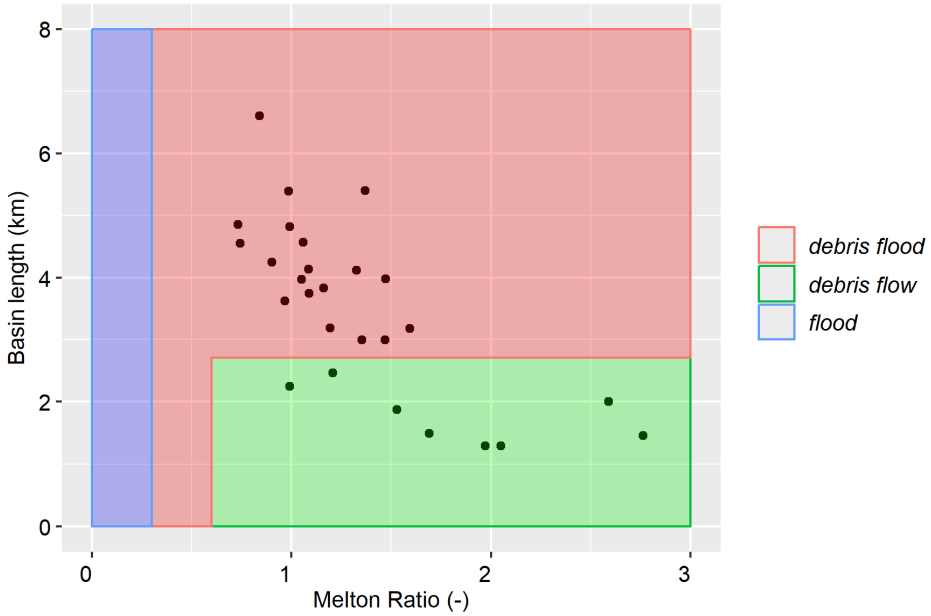

Figure 9. Catchment classification based on the hydrological and sediment transport processes using the discriminating limits of the different categories according to Wilford et al. (2004) [97].

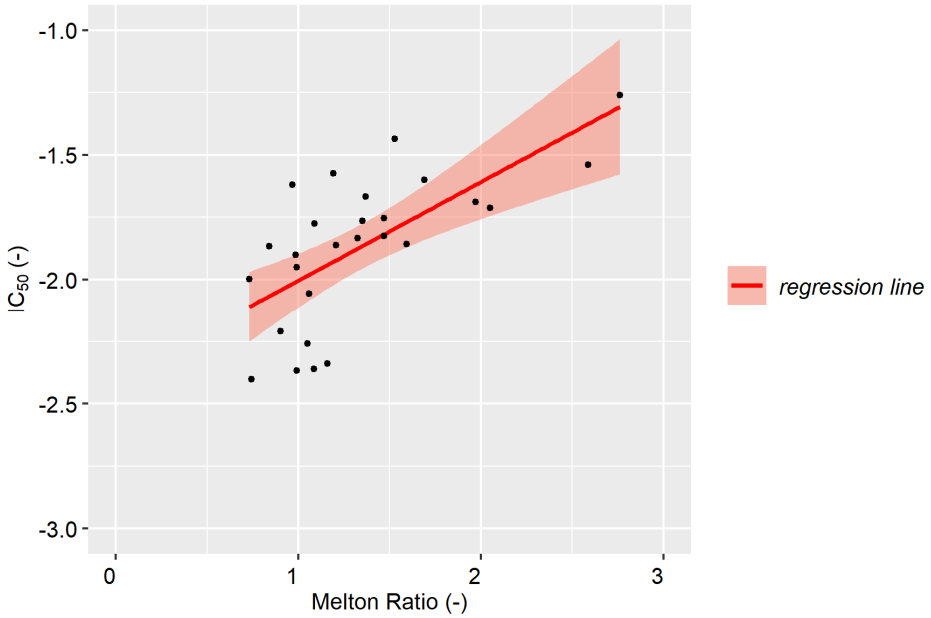

Figure 10. Relationships between the Melton Ratio and the mean value of connectivity index of all subcatchments of the study area.

4.2. Identification of Critical Areas

The diagnostic approach, including the integrated procedure HySEcA, provided qualitative and quantitative results that described the present conditions of the reaches (sediment, torrent control structures), and predicted the potential mobilized materials (water, sediment, and wood), a source of potential alterations along the watercourse. In the present study, the most evident morphological process was the estimation of high sediment production from the tributaries, and the aggradation of the gravel streambed. The deposition of gravel materials and the presence of several transverse torrent control structures that alter the slope of the streambed increased the level of flood risk and limited the watercourse dynamics. In addition to an overall assessment of the surveyed watercourse, the HySEcA included a more detailed assessment at reach scale. Such results can be simplified through discrete metrics (low, medium, and high) that evaluate the impacts of the main processes on the flood hazard (Table 7) inflow from the tributaries, erosion/deposition, and presence of obstacles. The upstream reach (4A), in proximity of the confluence between Adda River and Frodolfo Torrent, was identified as the most critical stretch of the watercourse, due to the observed significant aggradation of the streambed, the high input of sediment and large wood materials from the tributaries, and the limited sediment transport capacity. Other critical reaches were 4C, 4D and 6B, which showed an excess of deposited materials inside the channel and a relevant presence of obstacles.

Table 7. The synthesis of the HySEcA application according to the surveyed reaches: inflow includes the potential impacts of the quantity of water, sediment, and large wood during hydro-sedimentological events, morphological change represents the trajectory of torrent evolution in terms of deposition and erosion processes, and obstacles revels the dangerous presence of a specific elements (torrent control structures, stabilized sediments, large wood, or riparian vegetation).

Reach	Inflow	Morphological Change	Obstacles
4A	High	High	Low
4B	Low	Low	Medium
4C	Low	High	Medium
4D	Medium	High	Low
5A	Low	Medium	Medium
5B	Medium	Low	Low
5C	Medium	Low	Medium
5D	High	Low	Low
6A	Low	Medium	Low
6B	Low	High	Medium
6C	Low	High	Low
7A	Low	Medium	Low
7B	Low	Low	Low
8A	High	Low	Low

4.3. Advantages and Disadvantages

The HySEcA application, as a diagnostic approach, offers several advantages. First, the method aims to overcome the fragmentation and incompleteness of databases, organized and updated by local and regional authorities. The step-by-step procedure provides a sort of comprehensive list of variables (i.e., landscape elements) to monitor, such as streamflows, sediments, riparian vegetation, and torrent control structures. This approach promotes the reorganization and standardization of data, effectively forcing the unification and merging of databases essential for managing mountain fluvial environments. Second, HySEcA mainly focuses on the role of sediment transport in mountain catchments by providing both qualitative and quantitative estimates of its present impact of sediment transport on flood risk management. The methodology is a compromise between the availability of accessible data and the use of recent scientific approaches. The purpose is to obtain valid results on the active processes along the watercourse and across the surrounding upslope areas. Thus, these representative and clear results, obtained without compromising

scientific rigor, are useful for a wide spectrum of professionals (fluvial manager, engineers, ecologists, etc.) for proposing, designing, and evaluating appropriate and alternative countermeasures to reduce flood risk according to different hazard scenarios.

However, the methodology has some drawbacks. The accuracy of predictive models depends heavily on the quality and resolution of available data. Furthermore, although HySEcA is based on several empirical formulations widely used in scientific literature and practice, these models were primarily developed for specific environmental conditions (mainly Alpine regions) and could be not generalized worldwide. Moreover, the approaches include uncertainties and significant margins of error. To ensure reliable accuracy, it is crucial to leverage all collected data and establish a procedure for continuously updating the diagnosis as new data from monitoring activities become available.

4.4. Management Prescriptions

The comprehensive diagnosis of the surveyed watercourse integrated with the supplementary field campaigns was the starting point for developing the SMP and for proposing and/or programming maintenance and monitoring actions. In the present study, the diagnostic framework verified the aggradation of riverbed in several reaches of the surveyed watercourse, and therefore the increase in the flood risk, and predicted a significant contribution of sediment and large wood from the tributaries, well connected with the main watercourse. In this context, the mitigation of flood risk could be pursued through multiple and complementary management prescriptions that aim to create appropriate conditions for restoring or rehabilitating morphological processes (e.g., sediment transport from upstream to downstream). Such actions are generally difficult to implement because the altimetric and planimetric watercourse evolution has been constrained by urbanization (longitudinal and transverse torrent control structures, bridges, bike path, etc.) and the natural dynamics have almost disappeared, significantly interrupting the hydro-sedimentological processes. For this reason, the diagnostic approach provides useful data to qualitatively investigate (and predict) the morphological dynamic equilibrium, well described by the Lane's theory or Lane's balance [98]. Lane stated that, under simplified assumptions, the channel equilibrium is reached when the sediment transport capacity, described by the product between Q (in $m^3\ s^{-1}$) and S_c (m m^{-1}), is comparable to the sediment load represented by the product between sediment discharge per unit cross-section width (Q_s in $m^3\ s^{-1}\ m^{-1}$) and a representative sediment size d_s (in m) as follows:

$$Q \cdot S_c \approx Q_s \cdot d_s \tag{18}$$

Lane's balance demonstrates how the channel may respond to a change in various parameters such as sediment load, channel geometry, channel slope, erosion resistance, and discharges, and which solutions could be more appropriate to reduce the lack of equilibrium. Then, the purpose of the channel equilibrium could be determined by calculating the longitudinal slope of the watercourse, by comparing it with the present condition, and by implementing a catchment-based strategy over the time. Indeed, the management prescriptions must integrate many approaches, because none of them individually can solve a complex problem. For example, in the present case study, the SMP must include the following:

i. Rehabilitate sediment transport capacity: the increase in the longitudinal slope of the main watercourse along specific reach, the reduction in the flow resistance, and/or the removal of transverse torrent control structures can contribute to the sediment transport reducing the streambed aggradation.
ii. Control of sediment supply: a reduction in the sediment supply entering the watercourse from the contributing subcatchments could be useful in impeding the deposition. Several measures can be implemented at the catchment scale, such as erosion control approaches (e.g., reforestation, soil bioengineering techniques on

the hillslope) or solutions to trap sediment upstream of the confluences with the tributaries (e.g., construction retention check dams, retention basin).

iii. Trapping sediment in specific reservoirs: the detection of accessible and already altered areas, where the settling and accumulation of the sediment can balance the surplus of sediment.

iv. Redistributing or removing excessive sediments: where necessary, mechanical excavations are a practical solution for reducing the streambed aggradation; however, they are be associated with measures of reactivation of morphological dynamics (creating bars and islands, reactivation of secondary streams).

Another aspect of the SMP relates to improving the efficiency and the effectiveness of the monitoring activities. In fact, a well-organized and systematic monitoring of the watercourse and of its main variables is indispensable due to the complexity of the phenomenon and the potential effects of both natural and anthropogenic disturbances that can exacerbate the geohazards. Thus, the SMP must include a sort of monitoring plan at different temporal and spatial scale (Figure 11):

i. Periodic monitoring: updating the DEM, the Morphological Quality Index, and the inventories of maintenance and excavation operations arranged by the hydraulic authority, assessing the functionality of existing defense works, and surveying surface granulometry and riparian vegetation.

ii. Post-event monitoring: collecting details that are as accurate as possible on the triggering meteorological events and the associated consequences along the main watercourse including flooded areas, damaged infrastructures, removed riparian vegetation, presence of obstructions, etc. This kind of monitoring is crucial not only to update the state of the watercourse and any river changes, but also to provide valuable information on the watercourse's dynamics during flood, debris flood or debris flow events.

iii. Continuous monitoring: for the sediment management, collecting data on source areas extension (the detection of unstable areas) over the hillslope and on sediment movement (suspended sediment and bedload) within the river network is necessary. Moreover, this monitoring could be associated with early warning system for the inhabitants.

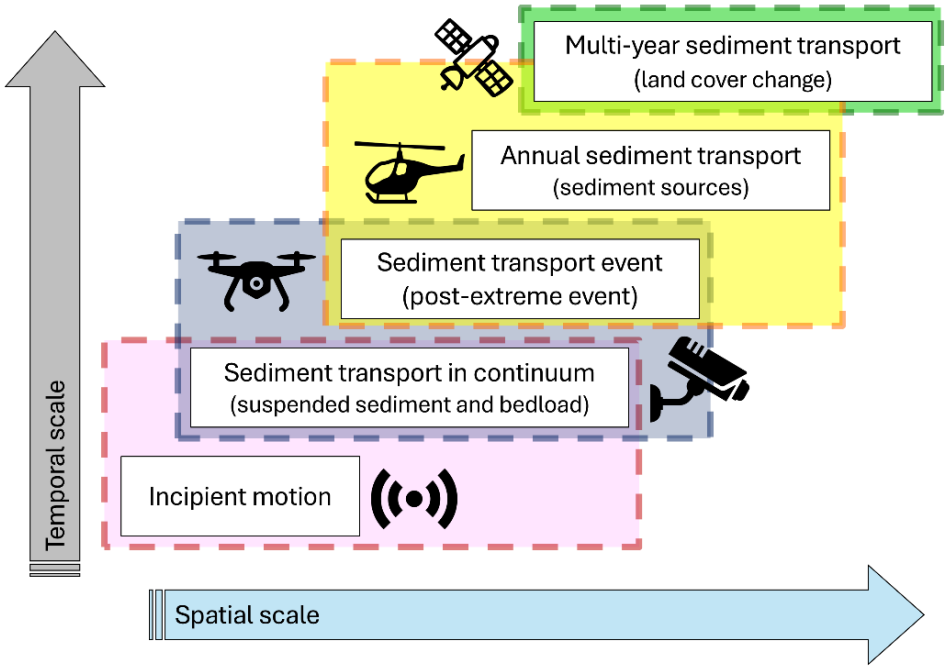

Figure 11. Flowchart of appropriate monitoring activities for integrating the sediment management plan.

5. Conclusions

The present study analyzed a mountain area, representative of the Alpine environment and subject to the impacts of tourism development and climate change. These territories showed a more frequent predisposition to flood, debris flood and debris flow events, and urgently require a robust strategy for controlling and handling the sediment transport within the catchment. The SMP is a crucial tool for planning and programming all those actions useful to improve the hydro-morphological efficiency, to conserve the riparian habitats, and to guarantee hydraulic safety for houses and infrastructures along the watercourse. Drafting a sustainable and modern SMP is a complex operation for the hydraulic authorities, as it requires a clear understanding (often holistic) of the present state of the catchment and of the watercourse, which is the result of collaboration between multiple skilled professionals and stakeholders. The procedure presented in this study aims to facilitate this work by ensuring scientific rigor and practical use, and by exploiting all the data already available to territorial authorities. The integrated HySEcA investigates all the key components of a mountain watercourse following the flux of sediments from the source, with a detailed approach to evaluating the inflows from the tributary subcatchments to the main hydrographic network, where erosion, transport, and deposition processes occur, and the interaction with existing torrent control structures and riparian vegetation is more significant. The proposed method was an innovative attempt to combine the scientific rigor and the availability of data and allowed us to reorganize the fragmented databases, to harmonize them across their different domains (topographic, geological, remote sensing, etc.), to integrate them with the field- and desk-based monitoring of the torrent control structures and of the riparian vegetation, and to provide (more than one) alternative future scenario(s) for effectively supporting the decision-making process. This analysis represents an example of how research experience from theory to practice can provide a robust and accurate evaluation considering the complexity of a mountain area.

Supplementary Materials: The following supporting information can be downloaded at: https://www.mdpi.com/article/10.3390/geohazards5040053/s1, Table A: Values of *CN* parameter, Table B: Values of *k* parameter, Table C: Values of *X* parameter, Table D: Values of *Y* parameter, and Table E: Values of ϕ parameter.

Author Contributions: Conceptualization, A.C. and G.B.B.; methodology, A.C., E.M. and G.B.B.; software, A.C., V.G.S. and D.B.; resources, G.B.B.; data curation, A.C., E.M., V.G.S. and D.B.; writing—original draft preparation, A.C. and E.M.; writing—review and editing, A.C., E.M. and G.B.B.; supervision, D.B.; project administration, G.B.B.; funding acquisition, G.B.B. All authors have read and agreed to the published version of the manuscript.

Funding: This research was funded by the project RETURN-PB (PNRR_BAC24ACISL_01), and by the scientific collaboration with Lombardy Region and Po River Basin Authority.

Data Availability Statement: The data presented in this study are available on request from the corresponding author.

Acknowledgments: This research was granted by the Local Authorities, Mountains, Energy Resources, Use of Water Resources Directorate of Lombardy Region (Italy) and by Po River Basin Authority. The authors wish to thank Mauro Visconti, Mario Domenico Zaffaroni, Nadia Chinaglia, Mauro Orlandi (Lombardy Region), Tommaso Simonelli, Margherita Agostini, Ginevra Mantovani (Po River Basin Authority), and Alessandro Loda (Regional Environmental Protection Agency) for their support.

Conflicts of Interest: The authors declare no conflicts of interest. The funders had no role in the design of the study; in the collection, analyses, or interpretation of data; in the writing of the manuscript; or in the decision to publish the results.

References

1. Piégay, H.; Darby, S.E.; Mosselman, E.; Surian, N. A Review of Techniques Available for Delimiting the Erodible River Corridor: A Sustainable Approach to Managing Bank Erosion. *River Res. Appl.* **2005**, *21*, 773–789. [CrossRef]
2. Keiler, M.; Knight, J.; Harrison, S. Climate Change and Geomorphological Hazards in the Eastern European Alps. *Philos. Trans. R. Soc. A.* **2010**, *368*, 2461–2479. [CrossRef]
3. Begert, M.; Frei, C. Long-term Area-mean Temperature Series for Switzerland—Combining Homogenized Station Data and High Resolution Grid Data. *Int. J. Clim.* **2018**, *38*, 2792–2807. [CrossRef]
4. Kotlarski, S.; Gobiet, A.; Morin, S.; Olefs, M.; Rajczak, J.; Samacoïts, R. 21st Century Alpine Climate Change. *Clim. Dyn.* **2023**, *60*, 65–86. [CrossRef]
5. Williamson, S.N.; Zdanowicz, C.; Anslow, F.S.; Clarke, G.K.C.; Copland, L.; Danby, R.K.; Flowers, G.E.; Holdsworth, G.; Jarosch, A.H.; Hik, D.S. Evidence for Elevation-Dependent Warming in the St. Elias Mountains, Yukon, Canada. *J. Clim.* **2020**, *33*, 3253–3269. [CrossRef]
6. Mancini, D.; Lane, S.N. Changes in Sediment Connectivity Following Glacial Debuttressing in an Alpine Valley System. *Geomorphology* **2020**, *352*, 106987. [CrossRef]
7. Micheletti, N.; Lane, S.N. Water Yield and Sediment Export in Small, Partially Glaciated Alpine Watersheds in a Warming Climate. *Water Resour. Res.* **2016**, *52*, 4924–4943. [CrossRef]
8. Liébault, F.; Piégay, H. Assessment of Channel Changes Due to Long-Term Bedload Supply Decrease, Roubion River, France. *Geomorphology* **2001**, *36*, 167–186. [CrossRef]
9. Ashmore, P. Channel Morphology and Bed Load Pulses in Braided, Gravel-Bed Streams. *Geogr. Ann. Ser. A Phys. Geogr.* **1991**, *73*, 37–52. [CrossRef]
10. Scorpio, V.; Surian, N.; Cucato, M.; Dai Prá, E.; Zolezzi, G.; Comiti, F. Channel Changes of the Adige River (Eastern Italian Alps) over the Last 1000 Years and Identification of the Historical Fluvial Corridor. *J. Maps* **2018**, *14*, 680–691. [CrossRef]
11. Curry, A.M.; Cleasby, V.; Zukowskyj, P. Paraglacial Response of Steep, Sediment-mantled Slopes to Post-'Little Ice Age' Glacier Recession in the Central Swiss Alps. *J. Quat. Sci.* **2006**, *21*, 211–225. [CrossRef]
12. Kondolf, G.M.; Piégay, H.; Landon, N. Channel Response to Increased and Decreased Bedload Supply from Land Use Change: Contrasts between Two Catchments. *Geomorphology* **2002**, *45*, 35–51. [CrossRef]
13. Guillon, H.; Mugnier, J.; Buoncristiani, J. Proglacial Sediment Dynamics from Daily to Seasonal Scales in a Glaciated Alpine Catchment (Bossons Glacier, Mont Blanc Massif, France). *Earth Surf. Process. Landf.* **2018**, *43*, 1478–1495. [CrossRef]
14. Piermattei, L.; Heckmann, T.; Betz-Nutz, S.; Altmann, M.; Rom, J.; Fleischer, F.; Stark, M.; Haas, F.; Ressl, C.; Wimmer, M.H.; et al. Evolution of an Alpine Proglacial River during 7 Decades of Deglaciation. *Earth Surf. Dyn.* **2023**, *11*, 383–403. [CrossRef]
15. Scorpio, V.; Cavalli, M.; Steger, S.; Crema, S.; Marra, F.; Zaramella, M.; Borga, M.; Marchi, L.; Comiti, F. Storm Characteristics Dictate Sediment Dynamics and Geomorphic Changes in Mountain Channels: A Case Study in the Italian Alps. *Geomorphology* **2022**, *403*, 108173. [CrossRef]
16. Antoniazza, G.; Nicollier, T.; Boss, S.; Mettra, F.; Badoux, A.; Schaefli, B.; Rickenmann, D.; Lane, S.N. Hydrological Drivers of Bedload Transport in an Alpine Watershed. *Water Resour. Res.* **2022**, *58*, e2021WR030663. [CrossRef]
17. Savi, S.; Pitscheider, F.; Engel, M.; Coviello, V.; Strecker, M.R.; Comiti, F. Sediment Export from an Alpine Proglacial Area under a Changing Climate: Budgets, Rates, and Geomorphological Processes. *Geomorphology* **2024**, *462*, 109343. [CrossRef]
18. Apitz, S.; White, S. A Conceptual Framework for River-Basin-Scale Sediment Management. *J. Soils Sediments* **2003**, *3*, 132–138. [CrossRef]
19. Rinaldi, M.; Simoncini, C.; Piégay, H. Scientific Design Strategy for Promoting Sustainable Sediment Management: The Case of the Magra River (Central-Northern Italy). *River Res. Appl.* **2009**, *25*, 607–625. [CrossRef]
20. Carladous, S.; Piton, G.; Tacnet, J.-M.; Philippe, F.; Nepote-Vesino, R.; Quefféléan, Y.; Marco, O. From the Restoration of French Mountainous Areas to Their Global Management: Historical Overview of the Water and Forestry Administration Actions in Public Forests. In Proceedings of the 13th INTERPRAEVENT Conference, Lucerne, Switzerland, 30 May–2 June 2016; pp. 34–42.
21. Hübl, J. Conceptual Framework for Sediment Management in Torrents. *Water* **2018**, *10*, 1718. [CrossRef]
22. Scorpio, V.; Comiti, F.; Liébault, F.; Piegay, H.; Rinaldi, M.; Surian, N. Channel Changes over the Last 200 Years: A Meta Data Analysis on European Rivers. *Earth Surf. Process. Landf.* **2024**, *49*, 2651–2676. [CrossRef]
23. Rinaldi, M.; Surian, N.; Comiti, F.; Bussettini, M. A Method for the Assessment and Analysis of the Hydromorphological Condition of Italian Streams: The Morphological Quality Index (MQI). *Geomorphology* **2013**, *180–181*, 96–108. [CrossRef]
24. Rinaldi, M.; Surian, N.; Comiti, F.; Bussettini, M. A Methodological Framework for Hydromorphological Assessment, Analysis and Monitoring (IDRAIM) Aimed at Promoting Integrated River Management. *Geomorphology* **2015**, *251*, 122–136. [CrossRef]
25. Brierley, G.J.; Fryirs, K.A. *Geomorphology and River Management: Applications of the River Styles Framework*; John Wiley & Sons: Hoboken, NJ, USA, 2013.
26. Perron, J.T.; Richardson, P.W.; Ferrier, K.L.; Lapôtre, M. The Root of Branching River Networks. *Nature* **2012**, *492*, 100–103. [CrossRef]
27. Kwang, J.S.; Langston, A.L.; Parker, G. The Role of Lateral Erosion in the Evolution of Nondendritic Drainage Networks to Dendricity and the Persistence of Dynamic Networks. *Proc. Natl. Acad. Sci. USA* **2021**, *118*, e2015770118. [CrossRef]
28. Fawen, L.; Qingyang, L.; Yong, Z. Characterization and Classification of River Network Types. *Water Resour. Manag.* **2023**, *37*, 6219–6236. [CrossRef]

29. Walley, Y.; Tunnicliffe, J.; Brierley, G. The Influence of Network Structure upon Sediment Routing in Two Disturbed Catchments, East Cape, New Zealand. *Geomorphology* **2018**, *307*, 38–49. [CrossRef]
30. Walley, Y.; Henshaw, A.J.; Brasington, J. Topological Structures of River Networks and Their Regional-scale Controls: A Multivariate Classification Approach. *Earth Surf. Process. Landf.* **2020**, *45*, 2869–2883. [CrossRef]
31. Montgomery, D.R.; Dietrich, W.E. Where Do Channels Begin? *Nature* **1988**, *336*, 232–234. [CrossRef]
32. Li, M.; Wu, B.; Chen, Y.; Li, D. Quantification of River Network Types Based on Hierarchical Structures. *CATENA* **2022**, *211*, 105986. [CrossRef]
33. Gaucherel, C.; Frelat, R.; Salomon, L.; Rouy, B.; Pandey, N.; Cudennec, C. Regional Watershed Characterization and Classification with River Network Analyses. *Earth Surf. Process. Landf.* **2017**, *42*, 2068–2081. [CrossRef]
34. Valjarević, A. GIS-Based Methods for Identifying River Networks Types and Changing River Basins. *Water Resour. Manag.* **2024**, *38*, 5323–5341. [CrossRef]
35. Bischetti, G.B.; Gandolfi, C.; Whelan, M.J. The Definition of Stream Channel Head Location Using Digital Elevation Data. In Proceedings of the HeadWater '98 Conference, Merano, Italy, 20–23 April 1998; Volume IAHS Publ. no. 248, pp. 545–552.
36. Montgomery, D.R.; Dietrich, W.E. Source Areas, Drainage Density, and Channel Initiation. *Water Resour. Res.* **1989**, *25*, 1907–1918. [CrossRef]
37. Tarolli, P.; Dalla Fontana, G. Hillslope-to-Valley Transition Morphology: New Opportunities from High Resolution DTMs. *Geomorphology* **2009**, *113*, 47–56. [CrossRef]
38. Montgomery, D.R.; Dietrich, W.E. Channel Initiation and the Problem of Landscape Scale. *Science* **1992**, *255*, 826–830. [CrossRef]
39. Bull, W.B. The Alluvial-Fan Environment. *Prog. Phys. Geogr. Earth Environ.* **1977**, *1*, 222–270. [CrossRef]
40. Harvey, A.M.; Mather, A.E.; Stokes, M. Introduction. A Review of Alluvial-Fan Research. In *Alluvial Fans: Geomorphology, Sedimentology, Dynamics*; Geological Society: London, UK, 2005; Volume 251, pp. 1–7. [CrossRef]
41. Norini, G.; Zuluaga, M.C.; Ortiz, I.J.; Aquino, D.T.; Lagmay, A.M.F. Delineation of Alluvial Fans from Digital Elevation Models with a GIS Algorithm for the Geomorphological Mapping of the Earth and Mars. *Geomorphology* **2016**, *273*, 134–149. [CrossRef]
42. Schwanghart, W.; Kuhn, N.J. TopoToolbox: A Set of Matlab Functions for Topographic Analysis. *Environ. Model. Softw.* **2010**, *25*, 770–781. [CrossRef]
43. Athira, P.; Sudheer, K.P.; Cibin, R.; Chaubey, I. Predictions in Ungauged Basins: An Approach for Regionalization of Hydrological Models Considering the Probability Distribution of Model Parameters. *Stoch. Environ. Res. Risk Assess.* **2016**, *30*, 1131–1149. [CrossRef]
44. Blöschl, G. Rainfall-Runoff Modeling of Ungauged Catchments. In *Encyclopedia of Hydrological Sciences*; Anderson, M.G., Ed.; John Wiley & Sons, Ltd.: Hoboken, NJ, USA, 2005; pp. 1–19.
45. Burlando, P.; Rosso, R. Scaling and Multiscaling Models of Depth-Duration-Frequency Curves for Storm Precipitation. *J. Hydrol.* **1996**, *187*, 45–64. [CrossRef]
46. Chiarelli, D.D.; Galizzi, M.; Bocchiola, D.; Rosso, R.; Rulli, M.C. Modeling Snowmelt Influence on Shallow Landslides in Tartano Valley, Italian Alps. *Sci. Total Environ.* **2023**, *856*, 158772. [CrossRef]
47. Nageswara Rao, K. Analysis of Surface Runoff Potential in Ungauged Basin Using Basin Parameters and SCS-CN Method. *Appl. Water Sci.* **2020**, *10*, 47. [CrossRef]
48. Merizalde, M.J.; Muñoz, P.; Corzo, G.; Muñoz, D.F.; Samaniego, E.; Célleri, R. Integrating Geographic Data and the SCS-CN Method with LSTM Networks for Enhanced Runoff Forecasting in a Complex Mountain Basin. *Front. Water* **2023**, *5*, 1233899. [CrossRef]
49. Mishra, S.K.; Singh, V.P. *Soil Conservation Service Curve Number (SCS-CN) Methodology*; Water Science and Technology Library; Springer: Dordrecht, The Netherlands, 2003; Volume 42, ISBN 978-90-481-6225-3.
50. Caletka, M.; Šulc Michalková, M.; Karásek, P.; Fučík, P. Improvement of SCS-CN Initial Abstraction Coefficient in the Czech Republic: A Study of Five Catchments. *Water* **2020**, *12*, 1964. [CrossRef]
51. Mishra, S.K.; Sahu, R.K.; Eldho, T.I.; Jain, M.K. An Improved Ia-S Relation Incorporating Antecedent Moisture in SCS-CN Methodology. *Water Resour. Manag.* **2006**, *20*, 643–660. [CrossRef]
52. Del Giudice, G.; Padulano, R.; Rasulo, G. Spatial Prediction of the Runoff Coefficient in Southern Peninsular Italy for the Index Flood Estimation. *Hydrol. Res.* **2014**, *45*, 263–281. [CrossRef]
53. Geetha, K.; Mishra, S.K.; Eldho, T.I.; Rastogi, A.K.; Pandey, R.P. Modifications to SCS-CN Method for Long-Term Hydrologic Simulation. *J. Irrig. Drain. Eng.* **2007**, *133*, 475–486. [CrossRef]
54. Jain, M.K.; Mishra, S.K.; Suresh Babu, P.; Venugopal, K.; Singh, V.P. Enhanced Runoff Curve Number Model Incorporating Storm Duration and a Nonlinear Ia-S Relation. *J. Hydrol. Eng.* **2006**, *11*, 631–635. [CrossRef]
55. Huff, F.A. Time Distribution of Rainfall in Heavy Storms. *Water Resour. Res.* **1967**, *3*, 1007–1019. [CrossRef]
56. Grimaldi, S.; Petroselli, A.; Nardi, F. A Parsimonious Geomorphological Unit Hydrograph for Rainfall–Runoff Modelling in Small Ungauged Basins. *Hydrol. Sci. J.* **2012**, *57*, 73–83. [CrossRef]
57. Evangelista, G.; Woods, R.; Claps, P. Dimensional Analysis of Literature Formulas to Estimate the Characteristic Flood Response Time in Ungauged Basins: A Velocity-Based Approach. *J. Hydrol.* **2023**, *627*, 130409. [CrossRef]
58. Jowett, I.G. Hydraulic Geometry of New Zealand Rivers and Its Use as a Preliminary Method of Habitat Assessment. *Regul. Rivers: Res. Mgmt.* **1998**, *14*, 451–466. [CrossRef]
59. Leopold, L.B. Downstream Change of Velocity in Rivers. *Am. J. Sci.* **1953**, *251*, 606–624. [CrossRef]

60. Pilgrim, D.H. Travel Times and Nonlinearity of Flood Runoff from Tracer Measurements on a Small Watershed. *Water Resour. Res.* **1976**, *12*, 487–496. [CrossRef]
61. Pilgrim, D.H. Isochrones of Travel Time and Distribution of Flood Storage from a Tracer Study on a Small Watershed. *Water Resour. Res.* **1977**, *13*, 587–595. [CrossRef]
62. Haan, C.T.; Barfield, B.J.; Hayes, J.C. *Design Hydrology and Sedimentology for Small Catchments*; Elsevier: Amsterdam, The Netherlands, 1994; ISBN 0-12-312340-2.
63. McCuen, R.H. *Hydrologic Analysis and Design*, 2nd ed.; Pearson Education/Prentice Hall: Upper Saddle River, NJ, USA, 1998; ISBN 978-0-13-134958-2.
64. Grimaldi, S.; Petroselli, A.; Alonso, G.; Nardi, F. Flow Time Estimation with Spatially Variable Hillslope Velocity in Ungauged Basins. *Adv. Water Resour.* **2010**, *33*, 1216–1223. [CrossRef]
65. D'Agostino, V.; Cerato, M.; Coali, R. Extreme Events of Sediment Transport in the Eastern Trentino Torrents. In Proceedings of the INTERPRAEVENT 1996, Garmisch-Partenkirchen, Germany, 24–28 June 1996; Volume 1, pp. 377–386.
66. Franzi, L.; Bianco, G. A Statistical Method to Predict Debris Flow Deposited Volumes on a Debris Fan. *Phys. Chem. Earth Part C Sol. Terr. Planet. Sci.* **2001**, *26*, 683–688. [CrossRef]
67. Hampel, R. Geschiebewirtschaft in Wildbächen. *Wildbach Und Lawinenverbau* **1977**, *41*, 3–34.
68. Rickenmann, D. Empirical Relationships for Debris Flows. *Nat. Hazards* **1999**, *19*, 47–77. [CrossRef]
69. VanDine, D.F. Debris Flows and Debris Torrents in the Southern Canadian Cordillera. *Can. Geotech. J.* **1985**, *22*, 44–68. [CrossRef]
70. Marchi, L.; Brunetti, M.T.; Cavalli, M.; Crema, S. Debris-flow Volumes in Northeastern Italy: Relationship with Drainage Area and Size Probability. *Earth Surf. Process. Landf.* **2019**, *44*, 933–943. [CrossRef]
71. Gavrilović, S. Méthode de La Classification Des Bassins Torrentiels et Équations Nouvelles Pour Le Calcul Des Hautes Eaux et Du Débit Solide. *Vadopriveda* **1959**.
72. Milanesi, L.; Pilotti, M.; Clerici, A. Application of an Improved Version of the Erosion Potential Method in Alpine Areas. *Ital. J. Eng. Geol. Environ.* **2016**, *1*, 17–30. [CrossRef]
73. Comiti, F.; Lucía, A.; Rickenmann, D. Large Wood Recruitment and Transport during Large Floods: A Review. *Geomorphology* **2016**, *269*, 23–39. [CrossRef]
74. Bracken, L.J.; Turnbull, L.; Wainwright, J.; Bogaart, P. Sediment Connectivity: A Framework for Understanding Sediment Transfer at Multiple Scales. *Earth Surf. Process. Landf.* **2015**, *40*, 177–188. [CrossRef]
75. Hooke, J.; Souza, J. Challenges of Mapping, Modelling and Quantifying Sediment Connectivity. *Earth-Sci. Rev.* **2021**, *223*, 103847. [CrossRef]
76. Cislaghi, A.; Bischetti, G.B. Source Areas, Connectivity, and Delivery Rate of Sediments in Mountainous-Forested Hillslopes: A Probabilistic Approach. *Sci. Total Environ.* **2019**, *652*, 1168–1186. [CrossRef]
77. Hoffmann, T. Sediment Residence Time and Connectivity in Non-Equilibrium and Transient Geomorphic Systems. *Earth-Sci. Rev.* **2015**, *150*, 609–627. [CrossRef]
78. Wohl, E.; Brierley, G.; Cadol, D.; Coulthard, T.J.; Covino, T.; Fryirs, K.A.; Grant, G.; Hilton, R.G.; Lane, S.N.; Magilligan, F.J.; et al. Connectivity as an Emergent Property of Geomorphic Systems: Geomorphic Connectivity. *Earth Surf. Process. Landf.* **2018**, *44*, 4–26. [CrossRef]
79. Martini, L.; Cavalli, M.; Picco, L. Predicting Sediment Connectivity in a Mountain Basin: A Quantitative Analysis of the Index of Connectivity. *Earth Surf. Process. Landf.* **2022**, *47*, 1500–1513. [CrossRef]
80. Borselli, L.; Cassi, P.; Torri, D. Prolegomena to Sediment and Flow Connectivity in the Landscape: A GIS and Field Numerical Assessment. *CATENA* **2008**, *75*, 268–277. [CrossRef]
81. Cavalli, M.; Trevisani, S.; Comiti, F.; Marchi, L. Geomorphometric Assessment of Spatial Sediment Connectivity in Small Alpine Catchments. *Geomorphology* **2013**, *188*, 31–41. [CrossRef]
82. Cucchiaro, S.; Cavalli, M.; Vericat, D.; Crema, S.; Llena, M.; Beinat, A.; Marchi, L.; Cazorzi, F. Monitoring Topographic Changes through 4D-Structure-from-Motion Photogrammetry: Application to a Debris-Flow Channel. *Environ. Earth Sci.* **2018**, *77*, 632. [CrossRef]
83. Lane, S.N.; Richards, K.S.; Chandler, J.H. Developments in Monitoring and Modelling Small-scale River Bed Topography. *Earth Surf. Process. Landf.* **1994**, *19*, 349–368. [CrossRef]
84. Wechsler, S.P.; Kroll, C.N. Quantifying DEM Uncertainty and Its Effect on Topographic Parameters. *Photogramm. Eng. Remote Sens.* **2006**, *72*, 1081–1090. [CrossRef]
85. Wise, S.M. Effect of Differing DEM Creation Methods on the Results from a Hydrological Model. *Comput. Geosci.* **2007**, *33*, 1351–1365. [CrossRef]
86. Chappell, A.; Heritage, G.L.; Fuller, I.C.; Large, A.R.G.; Milan, D.J. Geostatistical Analysis of Ground-Survey Elevation Data to Elucidate Spatial and Temporal River Channel Change. *Earth Surf. Process. Landf.* **2003**, *28*, 349–370. [CrossRef]
87. Cislaghi, A.; Bischetti, G.B. Best Practices in Post-Flood Surveys: The Study Case of Pioverna Torrent. *J. Agric. Eng.* **2022**, *53*, 11. [CrossRef]
88. Fuller, I.C.; Large, A.R.G.; Milan, D.J. Quantifying Channel Development and Sediment Transfer Following Chute Cutoff in a Wandering Gravel-Bed River. *Geomorphology* **2003**, *54*, 307–323. [CrossRef]
89. Brasington, J.; Langham, J.; Rumsby, B. Methodological Sensitivity of Morphometric Estimates of Coarse Fluvial Sediment Transport. *Geomorphology* **2003**, *53*, 299–316. [CrossRef]

90. Bunte, K.; Abt, S.R. Sampling Frame for Improving Peeble Count Accuracy in Coarse Gravel-Bed Streams. *JAWRA J. Am. Water Resour. Assoc.* **2001**, *37*, 1001–1014. [CrossRef]
91. Wolman, M.G. A Method of Sampling Coarse River-bed Material. *EOS Trans. Am. Geophys. Union* **1954**, *35*, 951–956.
92. Cucchiaro, S.; Cazorzi, F.; Marchi, L.; Crema, S.; Beinat, A.; Cavalli, M. Multi-Temporal Analysis of the Role of Check Dams in a Debris-Flow Channel: Linking Structural and Functional Connectivity. *Geomorphology* **2019**, *345*, 106844. [CrossRef]
93. Cislaghi, A.; Morlotti, E.; Cucchiaro, S.; Morando, P.; Bischetti, G.B. Monitoring of Torrent Control Structures: An Integrated Approach from First-level Inspections to Maintenance Strategies. *J. Flood Risk Manag.* **2024**, e13011. [CrossRef]
94. Fogliata, P.; Cislaghi, A.; Sala, P.; Giupponi, L. An Ecological Analysis of the Riparian Vegetation for Improving the Riverine Ecosystem Management: The Case of Lombardy Region (North Italy). *Landsc. Ecol. Eng.* **2021**, *17*, 375–386. [CrossRef]
95. Melton, M.A. Correlation Structure of Morphometric Properties of Drainage Systems and Their Controlling Agents. *J. Geol.* **1958**, *66*, 442–460. [CrossRef]
96. Montgomery, D.R.; MacDonald, L.H. Diagnostic Approach to Stream Channel Assessment and Monitoring. *J. Am. Water Resour. Assoc.* **2002**, *38*, 1–16. [CrossRef]
97. Wilford, D.J.; Sakals, M.E.; Innes, J.L.; Sidle, R.C.; Bergerud, W.A. Recognition of Debris Flow, Debris Flood and Flood Hazard through Watershed Morphometrics. *Landslides* **2004**, *1*, 61–66. [CrossRef]
98. Lane, E.W. Design of Stable Channels. *Trans. Am. Soc. Civ. Eng.* **1955**, *120*, 1234–1260. [CrossRef]